DMD Fast Forward. Published on February 4, 2013 as DOI: 10.1124/dmd.112.050211
DMD Fast Forward. Published on February 4, 2013 as doi:10.1124/dmd.112.050211
This article has not been copyedited and formatted. The final version may differ from this version.

RNA-Sequencing Quantification of Hepatic Ontogeny and Tissue Distribution of mRNAs of Phase-II Enzymes in Mice

Hong Lu, Sumedha Gunewardena, Julia Y. Cui, Byunggil Yoo, Xiao-bo Zhong and Curtis D. Klaassen

Department of Pharmacology, SUNY Upstate Medical University, Syracuse, New York 13210 (H.L.); Department of Medicine, University of Kansas Medical Center, Kansas City, Kansas 66160 (J.Y.C., C.D.K.); Kansas Intellectual and Developmental Disabilities Research Center, University of Kansas Medical Center, Kansas City, Kansas 66160 (S.G., B.Y.); Department of Pharmaceutical Sciences, University of Connecticut School of Pharmacy, Storrs, Connecticut 06269 (X.B.Z)

Downloaded from dmd.aspetjournals.org at ASPET Journals on April 18, 2024

Copyright 2013 by the American Society for Pharmacology and Experimental Therapeutics.

DMD Fast Forward. Published on February 4, 2013 as DOI: 10.1124/dmd.112.050211
This article has not been copyedited and formatted. The final version may differ from this version.

Running Title: Hepatic ontogeny and tissue distribution of Phase-II enzymes

Corresponding author: Dr. Hong Lu, Department of Pharmacology, SUNY Upstate Medical University, Syracuse, NY 13210. Telephone: 315-464-7978; Fax: 315-464-8008; Email: luh@upstate.edu.

Number of text pages: 43

Number of figures: 11

Number of tables: 0

Number of references: 51

Number of words in Abstract: 244

Number of words in Introduction: 506

Number of words in Discussion: 1840

Abbreviations: AA, amino acid; ADME, absorption, distribution, metabolism, and excretion; As3mt, arsenic (+3 oxidation state) methyltransferase; Baat, Bile acid-CoA:amino acid *N*-acyltransferase; Bal, bile acid-CoA ligase; BPA, bisphenol A; Ccbl1, cysteine conjugate-beta lyase 1; Comt, catechol *O*-methyltransferase; Gclc, glutamate-cysteine ligase catalytic subunit; Gclm, glutamate-cysteine ligase modifier subunit; Ggt1, gamma-glutamyltransferase 1; Glyat, Glycine-*N*-acyltransferase; GH, growth hormone; GSH, glutathione; Gst, glutathione *S*-transferase; Mat1a, methionine adenosyltransferase 1a; Nat, *N*-acetyltransferase; Nnmt, Nicotinamide *N*-methyltransferase; Papss1, 3'-phosphoadenosine 5'-phosphosulfate synthase 1; RNA-seq, RNA-sequencing; Sult, sulfotransferase; Tpmt, thiopurine *S*-methyltransferase; Ugdh, UDP-glucose 6-dehydrogenase; Ugp2, UDP-glucose pyrophosphorylase 2; Ugt, uridine diphosphate-glucuronosyltransferase.

Downloaded from dmd.aspetjournals.org at ASPET Journals on April 18, 2024

DMD Fast Forward. Published on February 4, 2013 as DOI: 10.1124/dmd.112.050211
This article has not been copyedited and formatted. The final version may differ from this version.

Abstract

Phase-II conjugating enzymes play key roles in the metabolism of xenobiotics. In the present study, RNA-sequencing was used to elucidate hepatic ontogeny and tissue distribution of mRNA expression of all major known Phase-II enzymes, including enzymes involved in glucuronidation, sulfation, glutathione conjugation, acetylation, methylation, and amino acid conjugation, as well as enzymes for the synthesis of Phase-II co-substrates in male C57BL/6J mice. Livers from male C57BL/6J mice were collected at 12 ages from prenatal to adulthood. Many of these Phase-II enzymes were expressed at much higher levels in adult livers than perinatal livers, such as *Ugt1a6b*, *2a3*, *2b1*, *2b5*, *2b36*, *3a1*, *3a2*, *Gsta1*, *m1*, *p1*, *p2*, *z1*, *mGst1*, *Nat8*, *Comt*, *Nnmt*, *Baat*, *Ugdh*, and *Gclc*. In contrast, hepatic mRNA expression of a few Phase-II enzymes decreased during postnatal liver development, such as *mGst2*, *mGst3*, *Gclm*, and *Mat2a*. Hepatic expression of certain Phase-II enzymes peaked during adolescent stage, such as *Ugt1a1*, *Sult1a1*, *Sult1c2*, *Sult1d1*, *Sult2as*, *Sult5a1*, *Tpmt*, *Glyat*, *Ugp2*, and *Mat1a*. In adult mice, the total transcripts for Phase-II enzymes were comparable in liver, kidney, and small intestine; however, Individual Phase-II enzymes display marked tissue specificity among the three organs. In conclusion, this study, for the first time, unveils developmental changes in mRNA abundance of all major known Phase-II enzymes in mouse liver, as well as their tissue-specific expression in key drug-metabolizing organs. The age- and tissue-specific expression of Phase-II enzymes indicate that the detoxification of xenobiotics is highly regulated by age and cell type.

Downloaded from dmd.aspetjournals.org at ASPET Journals on April 18, 2024

DMD Fast Forward. Published on February 4, 2013 as DOI: 10.1124/dmd.112.050211
This article has not been copyedited and formatted. The final version may differ from this version.

Introduction

Liver, kidney, and intestine are the three major tissues involved in the absorption, distribution, metabolism, and elimination of xenobiotics. Phase-II conjugating enzymes, such as sulfotransferases (*SULTs*), uridine diphosphate-glucuronosyltransferases (*UGTs*), glutathione *S*-transferases (*Gsts*), *N*-acetyltransferase (*NAT*), catechol *O*-methyltransferase (*COMT*), and amino-acid conjugation enzymes play key roles in catalyzing the conjugation reaction of xenobiotics (Jancova et al., 2010). Phase-II conjugates usually have decreased biological activities. Moreover, products of most of these phase-II conjugation reactions, with the exception of methylation and acetylation, have markedly increased water solubility and are readily excreted from the body. Therefore, Phase-II conjugation reactions are generally considered as major inactivation and detoxification pathways for xenobiotics, although activation of certain xenobiotics by these Phase-II enzymes has been reported (Glatt, 2000; Regan et al., 2010). In addition to xenobiotics, Phase-II enzymes are also important in the biotransformation of endobiotics, such as steroid hormones, thyroid hormones, bilirubin, and bile acids (Jancova et al., 2010).

Many drug-processing genes undergo marked changes in expression during tissue development and maturation. Children and newborn animals are often more susceptible to the adverse effects of therapeutic drugs and environmental chemicals due to their immature capacity to metabolize and detoxify these chemicals (Blake et al., 2005; Hines, 2008; Funk et al., 2012). Elucidation of developmental changes in expression patterns of these Phase-II enzymes will help to understand the mechanism of ontogenic regulation of gene expression. Additionally, extrahepatic tissues, including

Downloaded from dmd.aspetjournals.org at ASPET Journals on April 18, 2024

DMD Fast Forward. Published on February 4, 2013 as DOI: 10.1124/dmd.112.050211
This article has not been copyedited and formatted. The final version may differ from this version.

intestine and kidney, also play key roles in determining the absorption, distribution, metabolism, and excretion (ADME) of xenobiotics (Krishna and Klotz, 1994). It is essential to understand the tissue-specific expression patterns of Phase-II enzymes among the 3 major tissues in ADME, namely liver, kidney, and small intestine. Therefore, the purpose of the present study was to elucidate ontogenic changes in mRNA expression of all major known Phase-II enzymes during liver development and the distribution of mRNA expression of these Phase-II enzymes in adult tissues of liver, kidney, and small intestine.

There is already some information about the ontogenic expression patterns and tissue distribution of certain Phase-II enzymes in mice, such as *Sults* (Alnouti and Klaassen, 2006) and *Gsts* (Knight et al., 2007; Cui et al., 2010). However, hepatic ontogenic changes in the mRNA expression of *Ugts*, *Nats*, methyltransferases, and amino acid conjugating enzymes remain unknown. Moreover, conventional mRNA-profiling methods cannot compare the real abundance of transcripts between various genes. In contrast, RNA-sequencing (RNA-seq) provides a “true-quantification” of transcript counts (Malone and Oliver, 2011). Therefore, the purpose of this study was to use RNA-seq technology, for the first time, to generate comprehensive information on the ontogenic mRNA expression of all major known Phase-II enzymes in liver, and the distribution of mRNAs of these genes in adult liver, kidney, and small intestine using mouse as a model in a quantitative mode. This information will provide a foundation for understanding the relative importance of various Phase-II enzymes and their subfamily members in xenobiotic metabolism in liver at different developmental stages, as well as in the three key tissues of ADME, namely liver, kidney, and small intestine in adulthood.

Downloaded from dmd.aspetjournals.org at ASPET Journals on April 18, 2024

DMD Fast Forward. Published on February 4, 2013 as DOI: 10.1124/dmd.112.050211
This article has not been copyedited and formatted. The final version may differ from this version.

Materials and Methods

***Animals*.** Eight-week old C57BL/6J breeding pairs of mice were purchased from The Jackson Laboratory (Bar Harbor, ME). They were housed according to the American Animal Association Laboratory Animal Care guidelines, and were bred under standard conditions at the University of Kansas Medical Center. Livers from offspring were collected at the following 12 ages: day -2 (GD17.5), 0 (right after birth and before the start of suckling), 1, 3, 5, 10, 15, 20, 25, 30, 45, and 60. Due to potential variations caused by the estrous cycle in maturing adult female mice, only male livers were used for this study (N=3 per age, randomly selected from multiple litters). For the study of tissue distribution, tissues of liver, kidney, and small intestine were collected from adult male mice at 60 days of age (N=2 per tissue). Tissues were frozen immediately in liquid nitrogen, and stored at -80°C before use.

***Total RNA Preparation*.** Total RNA from liver, kidney, and small intestine was isolated using RNAzol Bee reagent (Tel-Test Inc., Friendswood, TX) per the manufacturer's protocol. RNA concentrations were quantified using a NanoDrop Spectrophotometer (NanoDrop Technologies, Wilmington, DE) at a wavelength of 260 nm. Integrity of the total RNA samples was evaluated using an Agilent 2100 Bioanalyzer (Agilent Technologies Inc., Santa Clara, CA) and the samples with RNA integrity values above 7.0 were used for the following experiments.

***cDNA Library Preparation and RNA-Seq of Liver Ontogeny Samples*.** The cDNA libraries from all total RNA samples of livers of 12 ages of mice were prepared using an Illumina TruSeq RNA sample prep kit (Illumina, San Diego, CA). Three micrograms of total RNA were used per the RNA input recommendations of the manufacturer's

Downloaded from dmd.aspetjournals.org at ASPET Journals on April 18, 2024

DMD Fast Forward. Published on February 4, 2013 as DOI: 10.1124/dmd.112.050211
This article has not been copyedited and formatted. The final version may differ from this version.

protocol. The mRNAs were selected from the total RNAs by purifying the poly-A containing molecules using poly-T primers. The RNA fragmentation, first and second strand cDNA syntheses, end repair, adaptor ligation, and PCR amplification were performed per the manufacturer's protocol. Fragments of the cDNA library ranged from 220 to 500 bps with an average size at 280 bp (including 100 bp adapter sequences). The quality of cDNA libraries was validated using an Agilent 2100 Bioanalyzer (Agilent Technologies Inc., Santa Clara, CA) before sequencing by Genome Sequencing Facility at the University of Kansas Medical Center. Briefly, the cDNA libraries clustered onto a TruSeq paired-end flow cell and sequenced (2×100) using a TruSeq 200 cycle SBS kit (Illumina, San Diego, CA). For the initial run, a PhiX control was loaded on each flowcell as well as universal human reference RNA on 1 of the 16 lanes of the Illumina HiSeq2000 sequencer, and sequenced in parallel with other samples to ensure the data generated for each run are accurately calibrated during the image analysis and data analysis. In addition, the PhiX was spiked into each cDNA sample at approximately 1% as an internal quality control.

***RNA-seq Data Analysis*.** After the sequencing platform generated the sequencing images, the pixel-level raw data collection, image analysis, and base calling were performed by the RTA (Real Time Analysis) software on a Dell PC attached to the HiSeq2000 sequencer. The data were streamed off to the analysis server as the run was progressing. The BCL Converter converted the BCL (base calling) files to qseq files, and the qseq files were subsequently converted to FASTQ files for downstream analysis. The RNA-seq reads from the FASTQ files were mapped to the mouse reference genome (NCBI37/mm9) and the splice junctions were identified by TopHat.

Downloaded from dmd.aspetjournals.org at ASPET Journals on April 18, 2024

DMD Fast Forward. Published on February 4, 2013 as DOI: 10.1124/dmd.112.050211
This article has not been copyedited and formatted. The final version may differ from this version.

The output files in BAM (binary sequence alignment) format were analyzed by Cufflinks to estimate the transcript abundance. The transcript structure predictions of Cufflinks are compared to Ensembl GTF version 65 by Cuffcompare. RNA-seq generated an average of 175 million reads per sample, and more than 80% of the reads were mapped to the mouse reference genome (NCBI37/mm9) by TopHat (data not shown). The mRNA abundance of genes was estimated by Cufflinks. The mRNA abundance was expressed in FPKM (fragments per kilobase of exon per million reads mapped), which normalizes sequencing depths between different samples and sizes between different genes, allowing direct comparison of expression levels among different transcripts on a genome-wide scale.

***cDNA Library Preparation and RNA-Seq of Tissue Distribution Samples*.** The preparation of cDNA libraries of adult male liver, kidney, and small intestine and sequencing of these cDNA libraries were conducted by Beijing Genomic Institute (BGI). Beads with oligo(dT) were used to isolate poly(A) mRNA from total RNA. Fragmentation buffer was added for breaking mRNA to short fragments. Taking these short fragments (200-700 nucleotides) as templates, random hexamer primers were used to synthesize the first-strand cDNA. The second-strand cDNA was synthesized using buffer, dNTPs, RNase H and DNA polymerase I, respectively. Short fragments were purified with QiaQuick PCR extraction kit and resolved with EB buffer for end reparation and adding poly(A). After that, the short fragments were connected with sequencing adaptors. For amplification with PCR, suitable fragments were selected as templates with respect to the result of agarose gel electrophoresis. The resultant cDNA libraries were sequenced using Illumina HiSeq™ 2000. Images generated by sequencers were converted by base

Downloaded from dmd.aspetjournals.org at ASPET Journals on April 18, 2024

DMD Fast Forward. Published on February 4, 2013 as DOI: 10.1124/dmd.112.050211
This article has not been copyedited and formatted. The final version may differ from this version.

calling into nucleotide sequences, which were called raw reads and were stored in FASTQ format. After removal of poor-quality reads which contain adapters, unknown, or low quality bases from the raw reads, the resultant clean reads were mapped to the mouse reference genome (NCBI37/mm9) and the splice junctions were identified by TopHat. FPKM method was used to calculate mRNA abundance, which normalizes sequencing depths between different samples and sizes between different genes. For the study of tissue distribution, the mRNA abundance was expressed as ratio to value of liver, with that of liver set as 1.0.

Validation of RNA-seq Data with Real-Time PCR. The total RNAs of male mouse livers at 8 ages, day -2, 1, 5, 10, 20, 25, 45, and 60 (n=3 per age), were reverse-transcribed into cDNAs using the High Capacity cDNA Reverse Transcription Kit (Applied Biosystems, Foster City, CA). The cDNAs were used for real-time PCR quantification of mRNA expression of mGst3 and Nat8 using the iTaq™ Universal SYBR® Green Supermix and a MyiQ2 Real-Time PCR Detection System (Bio-Rad Laboratories, Hercules, CA). No single commonly-used housekeeping gene had consistent mRNA expression levels throughout liver development (RNA-seq data, not shown). In contrast, the average expression levels of two housekeeping genes, namely Gapdh and Ncu-g1 (an integral membrane protein of the lysosome), were found to be consistent throughout liver development (Lu et al., 2012). Thus, amounts of mRNAs were calculated using the comparative CT method, which determines the amount of target normalized to the geometric mean of Gapdh and Ncu-g1. Real-Time PCR primers for mGst3 and Nat8 were: mGst3_for, AGATGGCTGTCCTCTCTAAGG; mGst3_rev,

Downloaded from dmd.aspetjournals.org at ASPET Journals on April 18, 2024

DMD Fast Forward. Published on February 4, 2013 as DOI: 10.1124/dmd.112.050211
This article has not been copyedited and formatted. The final version may differ from this version.

ATATGCCCGTTCTCAGGATCT; Nat8_for, GGACTACAAACAGGTCGTGGA; Nat8_rev, GCATACAACAGCCAGGAACCA.

Statistics. Data are presented as mean ± standard error (SE). Differences between various groups were determined using ANOVA followed by post-hoc test, with significance set at $p \leq 0.05$. In the study of liver ontogeny, the FPKM values were log2 transformed to achieve normal distribution prior to ANOVA. The statistics of mRNA expression of Phase-II enzymes during liver development (RNA-seq data) is shown in Supplemental Table 1.

Hierarchical clustering of Phase-II conjugating enzymes was performed using Matlab (R2012b, The MathWorks Inc, Natick, MA). The data were standardized to have a zero mean and unit variance at a gene level before clustering. The Ward's method was used for the linkage function applied on a Euclidean distance matrix of pair-wise distances of gene expression.

Gene set enrichment analysis (GSEA) was carried out using Ingenuity Pathways Analysis (IPA, Ingenuity Systems, Fall 2012 (www.ingenuity.com)). IPA identifies significant networks, functions, canonical pathways, and associated transcription factors in a set of genes based on information gathered in the Ingenuity Pathway Knowledge Base (IPKB). The IPKB is an extensive repository of information on genes and gene products that interact with each other. The significance (p-value) of the identified networks, functions and canonical pathways was calculated using the right-tailed Fisher's Exact Test. This test measures the significance of the overlap between the input genes and the genes in a particular category in the IPKB, reflecting the statistical significance of the network, function or canonical pathway with respect to the input

Downloaded from dmd.aspetjournals.org at ASPET Journals on April 18, 2024

DMD Fast Forward. Published on February 4, 2013 as DOI: 10.1124/dmd.112.050211
This article has not been copyedited and formatted. The final version may differ from this version.

genes and the reference genes (all genes in the IPKB identified with the particular network, function or canonical pathway). The analysis was performed on 85 Phase-II genes. The selection criteria for an expressed gene were expression in at least one day measured by the presence of an FPKM value (≥1.0). Input genes for "gene set enrichment" were perinatal Phase-II genes (13 mapped and analyzed in IPA out of 13 in cluster), Adolescent Phase-II genes (14 mapped and analyzed in IPA out of 18 in cluster), and Adult Phase-II genes (46 mapped and analyzed in IPA out of 54 in cluster).

Downloaded from dmd.aspetjournals.org at ASPET Journals on April 18, 2024

DMD Fast Forward. Published on February 4, 2013 as DOI: 10.1124/dmd.112.050211
This article has not been copyedited and formatted. The final version may differ from this version.

Results

The total FPKM values of all mRNA transcripts determined by RNA-seq were very similar among livers from different ages of mice, and/or among the three adult mouse tissues of liver, kidney, and small intestine, which is consistent with the equal loading of total RNAs from these samples in RNA-seq. The RNA-seq data of ontogenic mRNA expression in livers of C57BL/6J mice were highly quantitative, which had been validated in our previous studies (Cui et al., 2012; Lu et al., 2012; Peng et al., 2012). The raw data of FPKM values of RNA-seq data presented in this study are listed in Supplemental Tables 2 and 3.

Total Expression and Proportions of Individual Phase-II Enzymes during Liver Development in Male C57BL/6J Mice. Messenger RNA expression of most Phase-II enzymes had marked ontogenic changes during liver development (Fig. 1). Total transcripts of *Ugts* in liver were low before birth, increased gradually after birth, and reached the highest levels of ~24-fold prenatal levels 60 d after birth (Fig.1A). Conversely, total transcripts of *Sults* in liver were low before birth, increased rapidly after birth, peaked at 20 d post birth, and gradually fell back to ~5-fold prenatal levels 60 d after birth (Fig.1B). In contrast to the low pre-natal expression of *Ugts* and *Sults*, total transcripts of *Gsts* in liver were already high before birth, further increased gradually after birth, and plateaued at ~4-fold prenatal levels 30 d after birth (Fig.1C). Total transcripts of *Nats* (Nat1, 2, & 8) in liver were low before birth, slightly increased during postnatal development, started to surge after Day 25 (weaning), and reached the highest levels at adulthood (Day 60, Fig. 1D). Compared to *Nats*, total transcripts of methyltransferases in liver were more abundant, and the post-natal surge started at

Downloaded from dmd.aspetjournals.org at ASPET Journals on April 18, 2024

DMD Fast Forward. Published on February 4, 2013 as DOI: 10.1124/dmd.112.050211
This article has not been copyedited and formatted. The final version may differ from this version.

earlier time of Day 20 (before weaning), reached high levels at Day 30, and only increased slightly thereafter (Fig. 1E). Hepatic total transcripts of enzymes involved in amino acid (AA) conjugation of xenobiotics were low before birth, rapidly increased during perinatal stages, and reached adult levels after weaning (Day 25, Fig. 1F).

Hierarchical clustering revealed three distinct patterns of expression of Phase-II conjugating enzymes in liver with age (Fig. 2). Of the 87 enzymes involved in Phase-II conjugation, 84 genes were significantly expressed during different stages of liver development. The first cluster consisting of 13 genes expressed maximally between pre-natal day 2 (Day -2) and post-natal Day 5, and thus was categorized as perinatal-predominant Phase-II conjugating enzymes. The second cluster of 18 genes whose expression were maximum between Day 5 and Day 25 was categorized as adolescent-predominant Phase-II conjugating enzymes. The third cluster of 53 genes with maximum expression between day 25 and day 60 was identified as adult-predominant Phase-II conjugating enzymes. It was observed that genes in different groups of Phase-II conjugating enzymes were very selectively distributed among these three clusters (Chi-square test of independence; Yates' p-value 0.0032). For example, of the perinatal-predominant genes, 62% were equally distributed at 4 genes (31%) each between *Gsts* and co-substrate synthesizing enzymes. A majority of the adolescent-predominant genes were *Sults* (11 genes, 61%). Adult-predominant genes were mainly *Gsts* (19 genes, 35%) and *Ugts* (18 genes, 33%).

Among the main biological functions significantly associated with the perinatal-predominant Phase-II conjugating enzymes are metabolism of peptide, metabolism of glutathione, synthesis of glutathione, synthesis of S-adenosylmethionine, and

Downloaded from dmd.aspetjournals.org at ASPET Journals on April 18, 2024

DMD Fast Forward. Published on February 4, 2013 as DOI: 10.1124/dmd.112.050211
This article has not been copyedited and formatted. The final version may differ from this version.

cholestasis. Genes associated with adolescent-predominant Phase-II conjugating enzymes show significant function in sulfation of raloxifene, hormone, dopamine, 2-hydroxyestradiol and beta-estradiol, metabolism of estrogen, and steroid metabolism. The significant biological functions ascribed to the adult-predominant Phase-II conjugating enzymes include metabolism of xenobiotics, conjugation of glutathione, glucuronidation of hormone, glucuronidation of estrogen, metabolism of glutathione, glucuronidation of coumarin, conjugation of lipid, metabolism of peptide, glucuronidation of alcohol, etc.

***Hepatic Ontogeny of Ugt mRNAs in Male C57BL/6J Mice*.** Glucuronidation is critical for the metabolism and excretion of endogenous compounds and xenobiotics. The vast majority of *Ugt* family members displayed the adult-predominant expression pattern, with low expression before birth and gradual postnatal increase to the highest in adulthood (Fig. 3). A prominent change was a marked postnatal surge in hepatic expression of *Ugt1a1*, which peaked during adolescent stage and then decreased moderately at adulthood (Fig. 3A). In contrast, other Ugt1a subfamily members, including *Ugt1a5*, *Ugt1a6a*, *Ugt1a6b*, and *Ugt1a9*, all displayed adult-predominant expression pattern (Fig. 3A). Among *Ugt2a* subfamily, *Ugt2a3*, which catalyzes the glucuronidation of simple polycyclic aromatic hydrocarbons (Bushey et al., 2013), had adult-predominant expression pattern (Fig. 3A), whereas *Ugt2a1* and *2a2* were undetectable throughout liver development (data not shown). All the 7 *Ugt2b* subfamily members, namely *Ugt2b1*, *2b5*, *2b34*, *2b35*, *2b36*, *2b37*, and *2b38* all had adult-predominant expression patterns (Fig. 3A). *UGT3A1* is a UDP N-acetylglucosaminyltransferase with broad substrate activity toward ursodeoxycholic

Downloaded from dmd.aspetjournals.org at ASPET Journals on April 18, 2024

DMD Fast Forward. Published on February 4, 2013 as DOI: 10.1124/dmd.112.050211
This article has not been copyedited and formatted. The final version may differ from this version.

acid, 17alpha-estradiol, 17beta-estradiol, and the prototypic substrates of the *UGT1* and *UGT2* forms, 4-nitrophenol and 1-naphthol (Mackenzie et al., 2008). In contrast, *UGT3A2* uses UDP glucose and UDP xylose but not UDP N-acetylglucosamine to glycosidate a broad range of substrates including 4-methylumbelliferone, 1-hydroxypyrene, bioflavones, and estrogens (MacKenzie et al., 2011). Hepatic mRNA expression of *Ugt3a1* and *Ugt3a2* were very low before birth, increased gradually during postnatal development, and reached the highest levels at adulthood (Fig. 3A).

On Day -2 (2 d before birth), *Ugt2b34* was the most abundant *Ugt* isoform, followed by *Ugt2b35*, *2b36*, *1a6b*, and *2b5*; *Ugt1a1* only accounted for a very small percentage of total Ugts (Fig. 3B). On Day 1 (neonatal stage), due to a marked surge in *Ugt1a1* expression, *Ugt1a1* became the most abundant Ugt isoform, followed by *Ugt1a6b*, *2b34*, *2b35*, and *2b5*. On Day 25 (adolescent stage), due to marked increases in the expression of *Ugt2b* family members, *Ugt2b36* was the most abundant *Ugt* isoform, followed by *Ugt1a1*, *2b5*, and *1a6b*. On Day 60 (adulthood), *Ugt2b* family members, namely *Ugt2b5*, *2b36*, and *2b1* were the most abundant *Ugt* isoforms; however, many other *Ugt1a*, *2a*, and *3a* family members were also expressed at appreciable levels in adult liver (Fig. 3B). *Ugt8a*, an UDP-galactose:ceramide galactosyltransferase, was not expressed at any time during liver development (data not shown).

Hepatic Ontogeny of Sult mRNAs in Male C57BL/6J Mice. *Sult* family members had diverse ontogenic expression patterns during liver development (Fig. 4). *Sult1a1*, *1d1*, *1e1*, *2a1-2a6*, and *5a1* all displayed adolescent-predominant expression patterns (Fig. 4A). Hepatic mRNA expression of *Sult1c2* increased rapidly after birth, peaking at 5 d after birth, and then sharply decreased to low levels at 30 d of age. In contrast,

Downloaded from dmd.aspetjournals.org at ASPET Journals on April 18, 2024

DMD Fast Forward. Published on February 4, 2013 as DOI: 10.1124/dmd.112.050211
This article has not been copyedited and formatted. The final version may differ from this version.

hepatic expression of *Sult1b1,* which sulfonates dopamine and thyroid hormones (Saeki et al., 1998), reached the highest levels 15 d after birth and fluctuated thereafter (Fig. 4A). *Sult3a1*, *4a1*, and *6b1* transcripts remained undetectable throughout liver development in male mice (data not shown).

Before birth (Day -2), *Sult1a1,* which sulfonates phenolic compounds including steroid hormones, catecholamines, and phenolic drugs (Hempel et al., 2007), was the predominant *Sult* isoform in liver, accounting for >80% of total *Sult* transcripts (Fig. 4B). On Day 1, there were marked increases in the expression of steroid/bile acid sulfotransferase *Sult2a* (Huang et al., 2010) subfamily members, which account for >50% of total *Sult* transcripts in liver. A similar distribution in *Sult* isoforms were observed on Day 25, but with shrinking share for the *Sult1* family members. On Day 60, due to the silencing of most *Sult2a* subfamily genes, *Sult1a1* resumed as the predominant *Sult* isoform in liver, accounting for >80% *of total Sult transcripts*, followed by *Sult5a1*, *1d1*, and *1b1* (Fig. 4B).

***Hepatic Ontogeny of Gst mRNAs in Male C57BL/6J Mice*.** Various *Gst* subfamily members had distinct ontogenic expression patterns during liver development (Fig. 5). Members of *Gsta* subfamily all had adult-predominant expression patterns, with *Gsta3* being the predominant *Gsta* subfamily member, followed by *Gsta4* (Fig. 5A). *Gsta3* is essential for the protection of mice against DNA damage and hepatotoxicity induced by aflatoxin B1 (Ilic et al., 2010). Among the *Gstm* subfamily, *Gstm1* was the predominant isoform throughout liver development (Fig. 5A). *Gstm1* is essential for the protection of mice against methemoglobinemia induced by 1,2-dichloro-4-nitrobenzene through glutathione conjugation (Arakawa et al., 2010). *Gstm1*, *m4*, and *m6* had adult-

Downloaded from dmd.aspetjournals.org at ASPET Journals on April 18, 2024

DMD Fast Forward. Published on February 4, 2013 as DOI: 10.1124/dmd.112.050211
This article has not been copyedited and formatted. The final version may differ from this version.

predominant, *Gstm2* and *m3* had adolescent-predominant, *Gstm5* had fetal-predominant expression patterns, whereas *Gstm7* had no significant ontogenic changes (Fig. 5A). Among microsomal *Gst* (*mGst*) subfamily, there was a ontogenic switch during liver development: *mGst3* was the predominant *mGst* in fetal liver, whereas *mGst1* was the predominant *mGst* in adult liver, due to marked postnatal down-regulation of *mGst3* but increase of *mGst1* (Fig. 5A). Similar to *mGst3*, hepatic *mGst2* transcripts were markedly decreased during postnatal liver development. The most abundant *Gstt* subfamily was *Gstt1*, an enzyme essential for GSH conjugation of 1,2-epoxy-3-(p-nitrophenoxy)propane, dichloromethane, and the alkylating drug 1,3-bis(2-chloroethyl)-1-nitrosourea (Fujimoto et al., 2007). *Gstt1* and *Gstt3* had the adolescent-predominant expression pattern, whereas *Gstt2* mRNA expression surged one day after birth and then decreased to prenatal levels in adulthood (Fig. 5A). *Gstz1* is required for the metabolism of maleylacetoacetate (the penultimate step in the catabolism of phenylalanine and tyrosine) and alpha-halo acids, a carcinogenic contaminant of chlorinated water (Lim et al., 2004). *Gstp1/p2* play important and complicated roles in the metabolism of xenobiotics (Henderson and Wolf, 2011). *Gstz1*, *Gstp1*, and *Gstp2* had adult-predominant expression patterns, whereas mRNA expression of *Gsto1* fluctuated during postnatal liver development (Fig. 5A).

Before birth (Day -2), *mGst3* was the most abundant *Gst* in liver, followed by *Gstp1*, *t1*, and *m1* (Fig. 5B). On Day 1, *mGst1* replaced *mGst3* as the most abundant *Gst* isoform, followed by *Gsta3*, *z1*, and *p1*. On Day 25, *Gstm1* was the most abundant, followed by *mGst1*, *Gstt1*, and *Gsta3*. On Day 60, *Gstp1* and *mGst1* were the two most abundant Gsts, followed by *Gstm1* and *Gsta3* (Fig. 5B).

Downloaded from dmd.aspetjournals.org at ASPET Journals on April 18, 2024

DMD Fast Forward. Published on February 4, 2013 as DOI: 10.1124/dmd.112.050211
This article has not been copyedited and formatted. The final version may differ from this version.

***Hepatic Ontogeny of Nats, Methyltransferases, and Amino-acid Conjugating Enzymes in Male C57BL/6J Mice*.** Acetylation catalyzed by the arylamine *N*-acetyltransferases *Nat1*, *Nat2*, and *Nat3* is a major biotransformation pathway for arylamine and hydrazine drugs, as well as many carcinogens *(Sim et al., 2008)*. *Nat1* and *Nat2* mRNAs were expressed lowly before birth, and increased gradually during postnatal liver development, reached the highest levels at Day 60 (Fig. 6, top 1st panel). *Nat3* mRNAs were undetectable in mouse liver (data not shown). *Nat8* is a newly identified enzyme for mercapturic acid synthesis via acetylation of the cysteine *S*-conjugates (Veiga-da-Cunha et al., 2010). Hepatic mRNA expression of *Nat8* changed remarkably during development: *Nat8* mRNA was barely detectable through Day 25, and increased rapidly starting from Day 30, reaching the highest expression on Day 60.

Catechol-*O*-methyltransferase (*Comt*) catalyzes the methylation of large amount of phenolic compounds. Hepatic *Comt* mRNA was moderately expressed at Day -2 before birth, and surged during two stages of post-natal development: perinatal stage (from Day 1 to Day 3) and post-weaning stage (from Day 20 to Day 25) (Fig. 6, top 2nd panel). Nicotinamide *N*-methyltransferase (*Nnmt*) is a cytosolic enzyme that catalyzes the *N*-methylation of nicotinamide, pyridines, and other structural analogues (Aksoy et al., 1994). The most dramatic ontogenic change in methyltransferases was observed for *Nnmt*; hepatic *Nnmt* mRNA was very low until Day 10, thereafter it increased rapidly and reached a high level on Day 60 (Fig. 6, top 2nd panel). Arsenic (+3 oxidation state) methyltransferase (*As3MT*) is the arsenic methyltransferase that protects against arsenic toxicity by converting inorganic arsenic to the methylated metabolite (Sumi and Himeno, 2012). Hepatic *As3mt* mRNAs were moderately altered during development;

Downloaded from dmd.aspetjournals.org at ASPET Journals on April 18, 2024

DMD Fast Forward. Published on February 4, 2013 as DOI: 10.1124/dmd.112.050211
This article has not been copyedited and formatted. The final version may differ from this version.

As3mt mRNA was twice the amount in adult than fetal stage. Thiopurine *S*-methyltransferase (*Tpmt*) plays an important role in the metabolism and detoxification of some thiopurine drugs used in pediatric leukemia, rheumatoid arthritis, and inflammatory bowel disease (Mladosievicova et al., 2011). After birth, hepatic *Tpmt* mRNA gradually increased to the highest level on Day 15, and then slightly decreased to 3-fold the fetal level on Day 60 (Fig. 6, middle panel).

Bile acid-CoA ligase (*Bal*/*Slc27a5*) and bile acid-CoA:amino acid *N*-acyltransferase (*Baat*) are two key enzymes for conjugation of bile acids with glycine and taurine (Clayton, 2011). Glycine-*N*-acyltransferase (*Glyat*) catalyzes glycine conjugation, a Phase-II detoxification process for endogenous chemicals and xenobiotics, such as salicylic acid, benzoic acid, and methylbenzoic acid (Badenhorst et al., 2012). Before birth, *Bal* was already expressed moderately, and its expression was markedly increased during postnatal development, reaching the highest levels on Day 20, and fluctuated thereafter (Fig. 6, lower panel). Before birth, hepatic mRNA expression of *Baat* and *Glyat* was very low (Fig. 6, lower panel). After birth, these 2 AA conjugation enzymes was increased at different developmental stages: *Glyat* mRNA surged from Day 0 to Day 3 and increased to adult levels on Day 25. In contrast, hepatic *Baat* mRNA remained low until Day 10, after which it surged from Day 10 to Day 20, and maintained at high levels thereafter.

Gamma-glutamyltransferase 1 (*Ggt1*) plays a key role in gamma-glutamyl cycle, a pathway for the synthesis and degradation of glutathione as well as drug and xenobiotic detoxification. *Ggt1* catalyzes the formation of cysteine conjugates of xenobiotics. Cysteine conjugate-beta lyase 1 (*Ccbl1*) and *Ccbl2* catalyze the metabolism of cysteine

Downloaded from dmd.aspetjournals.org at ASPET Journals on April 18, 2024

DMD Fast Forward. Published on February 4, 2013 as DOI: 10.1124/dmd.112.050211
This article has not been copyedited and formatted. The final version may differ from this version.

conjugates of certain halogenated alkenes and alkanes, which often results in the formation of reactive metabolites leading to nephrotoxicity (Cooper and Pinto, 2006). Hepatic mRNA expression of *Ccbl1* fluctuated during the first 20 d of postnatal development, surged 4 fold from Day 20 to Day 25 (after weaning), and stayed constant thereafter (Fig. 6, bottom panel). In contrast, hepatic *Ccbl2* mRNA increased 23 fold from 2 d before birth (Day -2) to 1 d after birth (Day 1), and decreased markedly starting from Day 10, reaching Day 0 level at adulthood (Fig. 6, bottom panel).

Hepatic Ontogeny of mRNAs Encoding Enzymes Responsible for Synthesis of Co-substrates for Phase-II Conjugation Reactions in Male C57BL/6J Mice. UDP-glucose pyrophosphorylase 2 (*Ugp2*) catalyzes the synthesis of UDP-glucose, whereas UDP-glucose 6-dehydrogenase (*Ugdh*) converts UDP-glucose to UDP-glucuronate, the co-substrate for UDP-glucuronidation. Hepatic *Ugp2* mRNA increased 4 fold from Day -2 to Day 5, and slightly decreased after weaning (Day 25). In contrast, hepatic *Ugdh* mRNA expression did not increase until after weaning, and reached the highest level at adulthood (Day 60) (Fig. 7). 3'-Phosphoadenosine 5'-phosphosulfate synthase 1 (*Papss1*) and *Papss2* catalyze the synthesis of PAPS, the sulfate donor co-substrate for all sulfotransferases. Hepatic *Papss1* mRNA remained constantly low throughout development. In contrast, there was a Day 1 surge in hepatic *Papss2* mRNA, which peaked on Day 15 and slightly decreased thereafter. Glutamate-cysteine ligase catalytic (*Gclc*) and modifier (*Gclm*) subunit are enzymes for the synthesis of GSH, the co-substrate for all *Gsts*. Interestingly, hepatic *Gclc* mRNA increased, but *Gclm* mRNA decreased during liver maturation (Fig. 7).

Downloaded from dmd.aspetjournals.org at ASPET Journals on April 18, 2024

DMD Fast Forward. Published on February 4, 2013 as DOI: 10.1124/dmd.112.050211
This article has not been copyedited and formatted. The final version may differ from this version.

There was a marked ontogenic switch in hepatic expression of enzymes for the synthesis of the common methyl donor *S*-Adenosylmethionine: methionine adenosyltransferase 1a (*Mat1a*) expression increased markedly, whereas *Mat2a* and *Mat2b* mRNAs decreased moderately (48-68%) during postnatal development (Fig. 7).

Tissue Distribution of Phase-II Enzymes in Adult Liver, Kidney, and Small Intestine in Male C57BL/6J Mice. The 3 major tissues of drug processing, namely liver, kidney, and small intestine differed sharply in the expression of various Phase-II enzymes. In liver, *Ugt2b5*, *2b36*, and *2b1* were the most abundant *Ugts*. In kidney, *Ugt3a2*, *2b38*, and *3a1* accounted for more than 75% of total *Ugt* transcripts. In contrast, in small intestine, *Ugt2b34* accounted for more than 50% of total *Ugt* transcripts, followed by *Ugt2a3* and *1a7c* (Fig. 8A).

In liver, *Sult1a1* accounted for more than 65% of total *Sult* transcripts, followed by *Sult1d1* and *Sult5a1*. In kidney, *Sult1d1* accounted for more than 65% of total *Sult* transcripts, followed by *Sult1c2* and *Sult1a1*, with other *Sults* expressed lowly. In small intestine, 3 Sults, namely *Sult1b1*, *2b1*, and *1d1* accounted for almost all Sult transcripts (Fig. 8B).

Compared to *Ugts* and *Sults*, the expression of *Gst* family members was more diversified among the 3 tissues (Fig. 9). In liver, *mGst1*, *Gstp1*, *Gstm1*, and *Gsta3* were the most abundant *Gsts*. In kidney, *Gstm1*, *Gsta2*, *mGst3*, and *Gstz1* were the most abundant Gsts. In contrast, in small intestine, *Gsta1*, *Gstm3*, *mGst3*, and *Gsto1* were the most highly expressed *Gsts*.

The distribution of *Nat* mRNAs was less tissue-specific compared to other Phase-II enzymes. In all 3 tissues of liver, kidney, and small intestine, *Nat8* was the most

Downloaded from dmd.aspetjournals.org at ASPET Journals on April 18, 2024

DMD Fast Forward. Published on February 4, 2013 as DOI: 10.1124/dmd.112.050211
This article has not been copyedited and formatted. The final version may differ from this version.

abundant, followed by *Nat2* and *Nat1* (Data not shown). *Nat1* was only expressed in liver and kidney, *Nat2* was highest in small intestine, whereas *Nat8* was predominant in kidney (Fig. 10A). Regarding methyltransferases, *Comt* and *Nnmt* were liver-predominant, *Tpmt* was kidney-predominant, whereas *As3mt* expression was less variable among the 3 tissues (Fig. 10A).

Among the AA conjugation enzymes, *Bal* and *Baat* were highly liver-specific, whereas *Glyat* was only expressed in liver and kidney (Fig. 10B). *Ggt1* was only expressed in kidney and intestine, *Ccbl2* was liver-predominant, whereas *Ccbl1* was less variable among the 3 tissues (Fig. 10B).

The tissue distribution of enzymes for the synthesis of co-substrates was generally less variable compared to Phase-II enzymes (Fig. 10C). Tissues with the highest expression were: liver for *Ugp2*, *Gclc*, and *Mat1a*; kidney for *Gclm*, *Papss1*, *Mat2a*, and *Mat2b*; small intestine for *Ugdh* and *Papss2* (Fig. 10C).

***Real-time PCR Validation of RNA-seq Data*.** Consistent with RNA-seq data (Fig. 5A and 6), real-time PCR data showed that hepatic mRNA expression of *mGst3* was substantially down-regulated during postnatal development, whereas *Nat8* mRNA was barely detectable until Day 25, but surged from Day 25 to Day 60 (Fig. 11).

Downloaded from dmd.aspetjournals.org at ASPET Journals on April 18, 2024

DMD Fast Forward. Published on February 4, 2013 as DOI: 10.1124/dmd.112.050211
This article has not been copyedited and formatted. The final version may differ from this version.

Discussion

The present study, for the first time, provides comprehensive quantitative analysis of developmental regulation of mRNA expression of all major Phase-II enzymes, including enzymes involved in glucuronidation, sulfation, glutathione conjugation, acetylation, methylation, and AA conjugation in mouse liver. Many of these Phase-II enzymes display marked ontogenic changes in mRNA expression in liver, with a majority of them induced during postnatal liver development. In adulthood, these Phase-II enzymes have distinct expression levels in the three major tissues of drug processing, namely liver, kidney and small intestine.

The present data of hepatic ontogeny and tissue distribution of *Sults* are consistent with a previous report (Alnouti and Klaassen, 2006). Nevertheless, RNA-seq data illustrate the relative abundance of various *Sult* family members during liver development and among adult tissues, which were not known previously. It is noteworthy that although *Sult2a* isoforms are largely silenced in adult male mouse livers, they remain actively transcribed in adult female mouse livers (Alnouti and Klaassen, 2006). Additionally, although *Sult3a1* is not expressed in adult male mouse livers, it is expressed appreciably in livers of adult female mice (Alnouti and Klaassen, 2006).

The present data of hepatic ontogeny and tissue distribution of *Gsts* are largely consistent with previous reports (Knight et al., 2007; Cui et al., 2010), with the exception of *mGst3*. In the present study, results from both RNA-seq and real-time PCR showed that *mGst3* was the most abundant *Gsts* in mouse liver before birth, and *mGst3* was substantially down-regulated during postnatal liver development (Fig. 5A & Fig. 11). In

Downloaded from dmd.aspetjournals.org at ASPET Journals on April 18, 2024

DMD Fast Forward. Published on February 4, 2013 as DOI: 10.1124/dmd.112.050211
This article has not been copyedited and formatted. The final version may differ from this version.

contrast, a previous study showed that hepatic *mGst3* mRNA increased moderately (~1 fold) from Day -2 to Day 0, and remained unchanged thereafter (Cui et al., 2010). The reason of such apparent difference in hepatic ontogeny of *mGst3* in mice remains unclear, but appears unlikely due to strain difference, because both C57BL/6 mice were used in these 2 studies. In humans, *mGST3* mRNA expression is low in adult liver, but appears to be high in fetal liver (Jakobsson et al., 1997). Thus, apparently, both humans and mice have ontogenic down-regulation of *mGST3* during postnatal liver development. *mGst3* has been implicated in the synthesis of leukotriene C4 and possess glutathione-dependent peroxidase activity (Jakobsson et al., 1997).

The present study illustrates the first ontogenic patterns of mRNA expression of *Ugts* in mouse liver. Physiological functions change dramatically from fetal liver to adult liver. Adult liver is the major organ to metabolize amino acids and lipids, to maintain gluconeogenesis, to synthesize serum proteins, and to detoxify metabolic wastes and xenobiotics. In contrast, fetal liver has fewer metabolic functions and is a major organ for hematopoiesis. The perinatal surge of *Ugt1a1* is consistent with the key role of *Ugt1a1* in glucuronidation of bilirubin and prevention of hyperbilirubinemia (Kadakol et al., 2000). In contrast, the rapid increase in hepatic mRNA expression of many *Ugt2b* family members during weaning (Day 20 - Day 30) (Fig. 3) is consistent with their important role in the glucuronidation of steroid hormones and xenobiotics (Bock, 2010). *Ugp2* catalyzes the synthesis of UDP-glucose, whereas *Ugdh* converts UDP-glucose to UDP-glucuronate, the co-substrate for UDP-glucuronidation. UDP-glucose also serves as the precursor for glycogen synthesis. The increased need for glucuronidation of endogenous chemicals and the postnatal depletion of hepatic glycogen might be the

Downloaded from dmd.aspetjournals.org at ASPET Journals on April 18, 2024

DMD Fast Forward. Published on February 4, 2013 as DOI: 10.1124/dmd.112.050211
This article has not been copyedited and formatted. The final version may differ from this version.

driving force of the adolescent-predominant expression pattern of *Ugp2* (Fig. 7) whose expression decreases moderately after the replenish of glycogen storage in adolescent liver (Lopez et al., 1999). In contrast, the delayed surge in hepatic expression of *Ugdh* right after weaning (Fig. 7) coincides with marked increases in ingestion of xenobiotics and glucuronidation of these xenobiotics after weaning.

The present study, for the first time, illustrates ontogenic patterns of mRNA expression of Phase-II enzymes for acetylation and methylation in mouse liver. Hepatic mRNA expression of *Nats* involved in xenobiotic metabolism, such as *Nat1*, *Nat2*, and *Nat8*, are increased with liver maturation (Fig. 6). *Comt* is important in the metabolism of hormones (e.g. catecholamines and estrogens) and a large number of dietary phenolic compounds (Zhu, 2002). The two surges in *Comt* expression during perinatal (Day 1 to Day 3) and post-weaning (Day 20 to Day 25) might correspond to the markedly increased need for the metabolism of hormones and dietary phenolic compounds, respectively, during postnatal development. *Nnmt* catalyzes the *N*-methylation of nicotinamide, pyridines, and other structural analogues; its expression increases substantially with liver maturation. Interestingly, hepatic *NNMT* is markedly down-regulated in liver cancer patients (Kim et al., 2009). The regulatory mechanism of *Nnmt* expression during liver development and carcinogenesis warrants further investigation.

The present data suggest that neonatal mouse livers might differ considerably from adult livers regarding the metabolism of GSH conjugates. GSH conjugation is initiated by transfer of GSH onto an electrophilic acceptor (such as the anticancer drug cisplatin and toxicants ethylene dibromide and acrylamide), followed either by direct excretion of the GSH conjugates from the hepatocytes into bile, or by the hydrolysis of glutamate by

Downloaded from dmd.aspetjournals.org at ASPET Journals on April 18, 2024

DMD Fast Forward. Published on February 4, 2013 as DOI: 10.1124/dmd.112.050211
This article has not been copyedited and formatted. The final version may differ from this version.

Ggt to form cysteinyl-glycine-*S*-conjugates. Certain dipeptidases present in kidney and liver can hydrolyze the cysteinyl-glycine-*S*-conjugates to cysteine *S*-conjugates. *Nat8* catalyzes the acetylation of the cysteine *S*-conjugates in liver or kidney, leading to the formation of mercapturic acids, which are more polar and water-soluble than the original electrophiles and are readily excreted in urine or bile by multidrug resistance proteins. In the absence of acetylation, cysteinyl conjugates are unstable, undergoing β-elimination catalyzed by cysteine conjugate-β-lyase (*Ccbl*), with formation of toxic sulfur derivatives (Monks et al., 1990). Compared to adult mouse livers, the newborn mouse livers have much higher expression of *Ggt1* and *Ccbl2* (Fig. 7), but very low expression of *Nat8* (Fig. 6), which might result in a higher formation of toxic metabolites of certain GSH conjugates in newborns via the *Ggt-Ccbl2* β-elimination pathway.

RNA-seq provides the first genome-wide approach of true quantification of transcripts, which allows quantitative comparison of the abundance of various members within each gene family in various tissues. Such knowledge may be particularly useful for the study of the physiological function of a given Phase-II enzyme when using mice with targeted deletion of this gene. For example, *Sult1a1*, a major *Sult* with broad substrate specificity (Hempel et al., 2007), accounts for more than 60% of the total *Sult* transcripts in mouse liver, but only accounts for a very small percentage of total *Sult* transcripts in kidney and small intestine. Therefore, loss of *Sult1a1* is expected to markedly affect the sulfation of certain chemicals in liver, but may have minimal effect on the sulfation of these chemicals in kidney and small intestine. In contrast, loss of *Sult1d1* (a key enzyme for catecholamine sulfation) (Shimada et al., 2004) and *Ugt2b34* may markedly affect the sulfation and glucuronidation of chemicals in kidney and small intestine, respectively,

Downloaded from dmd.aspetjournals.org at ASPET Journals on April 18, 2024

DMD Fast Forward. Published on February 4, 2013 as DOI: 10.1124/dmd.112.050211
This article has not been copyedited and formatted. The final version may differ from this version.

because *Sult1d1* accounts for more than 70% of total *Sult* transcripts in kidney, whereas *Ugt2b34* accounts for more than 50% of total *Ugt* transcripts in small intestine.

It is noteworthy that only the mRNA levels of these Phase-II enzymes were investigated in this study. More studies are needed to determine whether the marked differences in mRNA expression of these Phase-II enzymes during different stages of liver development and among the three adult tissues of liver, kidney, and small intestine translate into differences in their protein expression and enzymatic function. Two recent genome-scale studies indicate that in mammalian cells, mRNA levels explain about 40% of the variation in protein levels (Schwanhausser et al., 2011); however, transcript levels correlate more strongly with clinical traits than protein levels (Ghazalpour et al., 2011). It is noteworthy that the ADME of xenobiotics depends on the cellular milieu composed of various transporters and metabolic enzymes coordinately regulated by a group of transcription factors (Klaassen and Slitt, 2005). Transcript levels of ADME genes might better reflect the cellular milieu for the ADME of xenobiotics under certain pathophysiological conditions. Bisphenol A (BPA) is an important industrial and environmental chemical. Phase-II conjugation reaction plays the key role in limiting the body's exposure to the parent unconjugated BPA, which is a well characterized endocrine disruptor (Taylor et al., 2011). Results from a comparative study on pharmacokinetics of BPA in neonatal and adult CD-1 mice demonstrate that neonatal mice (on Day 3 and Day 10) have much higher blood levels of unconjugated BPA than adult mice after oral ingestion. In contrast, post-weaning (Day 21) mice have blood levels of unconjugated BPA comparable to those in adult mice (Doerge et al., 2011). Glucuronidation is the major metabolic pathway for BPA in mice (Zalko et al., 2003). In

Downloaded from dmd.aspetjournals.org at ASPET Journals on April 18, 2024

DMD Fast Forward. Published on February 4, 2013 as DOI: 10.1124/dmd.112.050211
This article has not been copyedited and formatted. The final version may differ from this version.

parallel, the present data demonstrate that most *Ugts* are expressed lowly in neonatal mice (Day 3 and Day 10) but at high adult-comparable levels in post-weaning mice (Day 25). Thus, it appears that the marked differences in mRNA expression of these *Ugts* during different stages of liver development translate into differences in their protein expression and enzymatic function. Technological breakthroughs in proteomics and metabolomics are essential to conduct genome-scale comparative study to identify the sets of genes whose ontogenic expression are mainly regulated at transcriptional and posttranscriptional levels, respectively.

Although the mechanism of the ontogenic changes in hepatic expression of Phase-II enzymes is still unknown, literature suggest that growth hormone (GH) and androgens play key roles in the regulation of gender- and age-specific gene expression (Waxman and Holloway, 2009; Baik et al., 2011). The female- and male-predominant expression of *Ugt1a1* and *Ugt2b1*, respectively, in mouse liver is due to suppression of *Ugt1a1* mRNA but induction of *Ugt2b1* mRNA by male-pattern GH secretion (Buckley and Klaassen, 2009). Thus, the decrease in hepatic expression of *Ugt1a1* but induction of *Ugt2b1* in male mice upon puberty (after Day25, Fig. 3A) is likely due to the establishment of male-pattern GH secretion upon puberty. *Sult2a1/a2* has a markedly female-predominant expression in adult mouse liver due to suppressive effects of androgens and male-pattern GH secretion, as well as stimulatory effects by estrogens and female-pattern GH secretion (Alnouti and Klaassen, 2011). Thus, the marked hepatic down-regulation of *Sult2a1/2* and other *Sult2as* in male mice upon puberty (after Day25, Fig. 4A) may be due to the increase of androgens and establishment of male-pattern GH secretion upon puberty. Similarly, *Sult1a1* and *Sult1d1* have moderately

Downloaded from dmd.aspetjournals.org at ASPET Journals on April 18, 2024

DMD Fast Forward. Published on February 4, 2013 as DOI: 10.1124/dmd.112.050211
This article has not been copyedited and formatted. The final version may differ from this version.

female-predominant expression in adult mouse liver (Alnouti and Klaassen, 2006) due to suppressive effects of androgens and male-pattern GH secretion (Alnouti and Klaassen, 2011). Therefore, the moderate hepatic down-regulation of *Sult1a1* and *Sult1d1* in male mice upon puberty (after Day25, Fig. 4A) may be due to increase of androgens and establishment of male-pattern GH secretion upon puberty.

In summary, the present study provides the first knowledge about the true quantification of ontogenic patterns of mRNA expression of all major known Phase-II enzymes during mouse liver development and the distribution of these mRNAs among the three key tissues of ADME, namely liver, kidney, and small intestine in adulthood. Such knowledge will serve as the foundation for further study on the regulation of gene expression and physiological function of these Phase-II enzymes during liver development, as well as the mechanism of tissue-specific gene expression and the physiological importance of these Phase-II enzymes in these three key tissues of ADME.

Downloaded from dmd.aspetjournals.org at ASPET Journals on April 18, 2024

DMD Fast Forward. Published on February 4, 2013 as DOI: 10.1124/dmd.112.050211
This article has not been copyedited and formatted. The final version may differ from this version.

Acknowledgements

We thank Xiaohong Lei, Lai Peng, and Helen Renaud for technical assistance in animal experiments as well as Clark Bloomer from the KUMC Sequencing Core Facilities for his technical assistance in mRNA-seq.

Downloaded from dmd.aspetjournals.org at ASPET Journals on April 18, 2024

DMD Fast Forward. Published on February 4, 2013 as DOI: 10.1124/dmd.112.050211
This article has not been copyedited and formatted. The final version may differ from this version.

Authorship Contributions

Participated in research design: Lu, Yoo, Gunewardena, Zhong, and Klaassen.

Conducted experiments: Lu and Cui.

Performed data analysis: Lu, Cui, Gunewardena, and Yoo.

Wrote or contributed to the writing of the manuscript: Lu, Cui, Yoo, Gunewardena, Zhong, and Klaassen.

Downloaded from dmd.aspetjournals.org at ASPET Journals on April 18, 2024

DMD Fast Forward. Published on February 4, 2013 as DOI: 10.1124/dmd.112.050211
This article has not been copyedited and formatted. The final version may differ from this version.

References

Aksoy S, Szumlanski CL, and Weinshilboum RM (1994) Human liver nicotinamide N-methyltransferase. cDNA cloning, expression, and biochemical characterization. *J Biol Chem* **269:**14835-14840.

Alnouti Y and Klaassen CD (2006) Tissue distribution and ontogeny of sulfotransferase enzymes in mice. *Toxicol Sci* **93:**242-255.

Alnouti Y and Klaassen CD (2011) Mechanisms of gender-specific regulation of mouse sulfotransferases (Sults). *Xenobiotica* **41:**187-197.

Arakawa S, Maejima T, Kiyosawa N, Yamaguchi T, Shibaya Y, Aida Y, Kawai R, Fujimoto K, Manabe S, and Takasaki W (2010) Methemoglobinemia induced by 1,2-dichloro-4-nitrobenzene in mice with a disrupted glutathione S-transferase Mu 1 gene. *Drug Metab Dispos* **38:**1545-1552.

Badenhorst CP, Jooste M, and van Dijk AA (2012) Enzymatic characterization and elucidation of the catalytic mechanism of a recombinant bovine glycine N-acyltransferase. *Drug Metab Dispos* **40:**346-352.

Baik M, Yu JH, and Hennighausen L (2011) Growth hormone-STAT5 regulation of growth, hepatocellular carcinoma, and liver metabolism. *Ann N Y Acad Sci* **1229:**29-37.

Blake MJ, Castro L, Leeder JS, and Kearns GL (2005) Ontogeny of drug metabolizing enzymes in the neonate. *Semin Fetal Neonatal Med* **10:**123-138.

Bock KW (2010) Functions and transcriptional regulation of adult human hepatic UDP-glucuronosyl-transferases (UGTs): mechanisms responsible for interindividual variation of UGT levels. *Biochem Pharmacol* **80:**771-777.

Downloaded from dmd.aspetjournals.org at ASPET Journals on April 18, 2024

DMD Fast Forward. Published on February 4, 2013 as DOI: 10.1124/dmd.112.050211
This article has not been copyedited and formatted. The final version may differ from this version.

Buckley DB and Klaassen CD (2009) Mechanism of gender-divergent UDP-glucuronosyltransferase mRNA expression in mouse liver and kidney. *Drug Metab Dispos* **37:**834-840.

Bushey RT, Dluzen DF, and Lazarus P (2013) Importance of UDP-Glucuronosyltransferases 2A2 and 2A3 in Tobacco Carcinogen Metabolism. *Drug Metab Dispos* **41:**170-179.

Clayton PT (2011) Disorders of bile acid synthesis. *J Inherit Metab Dis* **34:**593-604.

Cooper AJ and Pinto JT (2006) Cysteine S-conjugate beta-lyases. *Amino Acids* **30:**1-15.

Cui JY, Choudhuri S, Knight TR, and Klaassen CD (2010) Genetic and epigenetic regulation and expression signatures of glutathione S-transferases in developing mouse liver. *Toxicol Sci* **116:**32-43.

Cui JY, Gunewardena SS, Yoo B, Liu J, Renaud HJ, Lu H, Zhong XB, and Klaassen CD (2012) RNA-Seq reveals different mRNA abundance of transporters and their alternative transcript isoforms during liver development. *Toxicol Sci* **127:**592-608.

Doerge DR, Twaddle NC, Vanlandingham M, and Fisher JW (2011) Pharmacokinetics of bisphenol A in neonatal and adult CD-1 mice: inter-species comparisons with Sprague-Dawley rats and rhesus monkeys. *Toxicol Lett* **207:**298-305.

Fujimoto K, Arakawa S, Watanabe T, Yasumo H, Ando Y, Takasaki W, Manabe S, Yamoto T, and Oda S (2007) Generation and functional characterization of mice with a disrupted glutathione S-transferase, theta 1 gene. *Drug Metab Dispos* **35:**2196-2202.

Downloaded from dmd.aspetjournals.org at ASPET Journals on April 18, 2024

DMD Fast Forward. Published on February 4, 2013 as DOI: 10.1124/dmd.112.050211
This article has not been copyedited and formatted. The final version may differ from this version.

Funk RS, Brown JT, and Abdel-Rahman SM (2012) Pediatric pharmacokinetics: human development and drug disposition. *Pediatr Clin North Am* **59:**1001-1016.

Ghazalpour A, Bennett B, Petyuk VA, Orozco L, Hagopian R, Mungrue IN, Farber CR, Sinsheimer J, Kang HM, Furlotte N, Park CC, Wen PZ, Brewer H, Weitz K, Camp DG, 2nd, Pan C, Yordanova R, Neuhaus I, Tilford C, Siemers N, Gargalovic P, Eskin E, Kirchgessner T, Smith DJ, Smith RD, and Lusis AJ (2011) Comparative analysis of proteome and transcriptome variation in mouse. *PLoS Genet* **7:**e1001393.

Glatt H (2000) Sulfotransferases in the bioactivation of xenobiotics. *Chem Biol Interact* **129:**141-170.

Hempel N, Gamage N, Martin JL, and McManus ME (2007) Human cytosolic sulfotransferase SULT1A1. *Int J Biochem Cell Biol* **39:**685-689.

Henderson CJ and Wolf CR (2011) Knockout and transgenic mice in glutathione transferase research. *Drug Metab Rev* **43:**152-164.

Hines RN (2008) The ontogeny of drug metabolism enzymes and implications for adverse drug events. *Pharmacol Ther* **118:**250-267.

Huang J, Bathena SP, Tong J, Roth M, Hagenbuch B, and Alnouti Y (2010) Kinetic analysis of bile acid sulfation by stably expressed human sulfotransferase 2A1 (SULT2A1). *Xenobiotica* **40:**184-194.

Ilic Z, Crawford D, Vakharia D, Egner PA, and Sell S (2010) Glutathione-S-transferase A3 knockout mice are sensitive to acute cytotoxic and genotoxic effects of aflatoxin B1. *Toxicol Appl Pharmacol* **242:**241-246.

Downloaded from dmd.aspetjournals.org at ASPET Journals on April 18, 2024

DMD Fast Forward. Published on February 4, 2013 as DOI: 10.1124/dmd.112.050211
This article has not been copyedited and formatted. The final version may differ from this version.

Jakobsson PJ, Mancini JA, Riendeau D, and Ford-Hutchinson AW (1997) Identification and characterization of a novel microsomal enzyme with glutathione-dependent transferase and peroxidase activities. *J Biol Chem* **272:**22934-22939.

Jancova P, Anzenbacher P, and Anzenbacherova E (2010) Phase II drug metabolizing enzymes. *Biomed Pap Med Fac Univ Palacky Olomouc Czech Repub* **154:**103-116.

Kadakol A, Ghosh SS, Sappal BS, Sharma G, Chowdhury JR, and Chowdhury NR (2000) Genetic lesions of bilirubin uridine-diphosphoglucuronate glucuronosyltransferase (UGT1A1) causing Crigler-Najjar and Gilbert syndromes: correlation of genotype to phenotype. *Hum Mutat* **16:**297-306.

Kim J, Hong SJ, Lim EK, Yu YS, Kim SW, Roh JH, Do IG, Joh JW, and Kim DS (2009) Expression of nicotinamide N-methyltransferase in hepatocellular carcinoma is associated with poor prognosis. *J Exp Clin Cancer Res* **28:**20.

Klaassen CD and Slitt AL (2005) Regulation of hepatic transporters by xenobiotic receptors. *Curr Drug Metab* **6:**309-328.

Knight TR, Choudhuri S, and Klaassen CD (2007) Constitutive mRNA expression of various glutathione S-transferase isoforms in different tissues of mice. *Toxicol Sci* **100:**513-524.

Krishna DR and Klotz U (1994) Extrahepatic metabolism of drugs in humans. *Clin Pharmacokinet* **26:**144-160.

Lim CE, Matthaei KI, Blackburn AC, Davis RP, Dahlstrom JE, Koina ME, Anders MW, and Board PG (2004) Mice deficient in glutathione transferase zeta/maleylacetoacetate isomerase exhibit a range of pathological changes and

Downloaded from dmd.aspetjournals.org at ASPET Journals on April 18, 2024

DMD Fast Forward. Published on February 4, 2013 as DOI: 10.1124/dmd.112.050211
This article has not been copyedited and formatted. The final version may differ from this version.

elevated expression of alpha, mu, and pi class glutathione transferases. *Am J Pathol* **165:**679-693.

Lopez MF, Dikkes P, Zurakowski D, Villa-Komaroff L, and Majzoub JA (1999) Regulation of hepatic glycogen in the insulin-like growth factor II-deficient mouse. *Endocrinology* **140:**1442-1448.

Lu H, Cui J, Gunewardena S, Yoo B, Zhong XB, and Klaassen C (2012) Hepatic ontogeny and tissue distribution of mRNAs of epigenetic modifiers in mice using RNA-sequencing. *Epigenetics* **7:**914-929.

MacKenzie PI, Rogers A, Elliot DJ, Chau N, Hulin JA, Miners JO, and Meech R (2011) The novel UDP glycosyltransferase 3A2: cloning, catalytic properties, and tissue distribution. *Mol Pharmacol* **79:**472-478.

Mackenzie PI, Rogers A, Treloar J, Jorgensen BR, Miners JO, and Meech R (2008) Identification of UDP glycosyltransferase 3A1 as a UDP N-acetylglucosaminyltransferase. *J Biol Chem* **283:**36205-36210.

Malone JH and Oliver B (2011) Microarrays, deep sequencing and the true measure of the transcriptome. *BMC Biol* **9:**34.

Mladosievicova B, Dzurenkova A, Sufliarska S, and Carter A (2011) Clinical relevance of thiopurine S-methyltransferase gene polymorphisms. *Neoplasma* **58:**277-282.

Monks TJ, Anders MW, Dekant W, Stevens JL, Lau SS, and van Bladeren PJ (1990) Glutathione conjugate mediated toxicities. *Toxicol Appl Pharmacol* **106:**1-19.

Peng L, Yoo B, Gunewardena SS, Lu H, Klaassen CD, and Zhong XB (2012) RNA sequencing reveals dynamic changes of mRNA abundance of cytochromes P450

Downloaded from dmd.aspetjournals.org at ASPET Journals on April 18, 2024

DMD Fast Forward. Published on February 4, 2013 as DOI: 10.1124/dmd.112.050211
This article has not been copyedited and formatted. The final version may differ from this version.

and their alternative transcripts during mouse liver development. *Drug Metab Dispos* **40:**1198-1209.

Regan SL, Maggs JL, Hammond TG, Lambert C, Williams DP, and Park BK (2010) Acyl glucuronides: the good, the bad and the ugly. *Biopharm Drug Dispos* **31:**367-395.

Saeki Y, Sakakibara Y, Araki Y, Yanagisawa K, Suiko M, Nakajima H, and Liu MC (1998) Molecular cloning, expression, and characterization of a novel mouse liver SULT1B1 sulfotransferase. *J Biochem* **124:**55-64.

Schwanhausser B, Busse D, Li N, Dittmar G, Schuchhardt J, Wolf J, Chen W, and Selbach M (2011) Global quantification of mammalian gene expression control. *Nature* **473:**337-342.

Shimada M, Terazawa R, Kamiyama Y, Honma W, Nagata K, and Yamazoe Y (2004) Unique properties of a renal sulfotransferase, St1d1, in dopamine metabolism. *J Pharmacol Exp Ther* **310:**808-814.

Sim E, Walters K, and Boukouvala S (2008) Arylamine N-acetyltransferases: from structure to function. *Drug Metab Rev* **40:**479-510.

Sumi D and Himeno S (2012) Role of arsenic (+3 oxidation state) methyltransferase in arsenic metabolism and toxicity. *Biol Pharm Bull* **35:**1870-1875.

Taylor JA, Vom Saal FS, Welshons WV, Drury B, Rottinghaus G, Hunt PA, Toutain PL, Laffont CM, and VandeVoort CA (2011) Similarity of bisphenol A pharmacokinetics in rhesus monkeys and mice: relevance for human exposure. *Environ Health Perspect* **119:**422-430.

Downloaded from dmd.aspetjournals.org at ASPET Journals on April 18, 2024

DMD Fast Forward. Published on February 4, 2013 as DOI: 10.1124/dmd.112.050211
This article has not been copyedited and formatted. The final version may differ from this version.

Veiga-da-Cunha M, Tyteca D, Stroobant V, Courtoy PJ, Opperdoes FR, and Van Schaftingen E (2010) Molecular identification of NAT8 as the enzyme that acetylates cysteine S-conjugates to mercapturic acids. *J Biol Chem* **285:**18888-18898.

Waxman DJ and Holloway MG (2009) Sex differences in the expression of hepatic drug metabolizing enzymes. *Mol Pharmacol* **76:**215-228.

Zalko D, Soto AM, Dolo L, Dorio C, Rathahao E, Debrauwer L, Faure R, and Cravedi JP (2003) Biotransformations of bisphenol A in a mammalian model: answers and new questions raised by low-dose metabolic fate studies in pregnant CD1 mice. *Environ Health Perspect* **111:**309-319.

Zhu BT (2002) Catechol-O-Methyltransferase (COMT)-mediated methylation metabolism of endogenous bioactive catechols and modulation by endobiotics and xenobiotics: importance in pathophysiology and pathogenesis. *Curr Drug Metab* **3:**321-349.

Downloaded from dmd.aspetjournals.org at ASPET Journals on April 18, 2024

DMD Fast Forward. Published on February 4, 2013 as DOI: 10.1124/dmd.112.050211
This article has not been copyedited and formatted. The final version may differ from this version.

Footnotes.

This work was supported by the National Institutes of Health National Institute of Environmental Health Sciences [Grant ES-019487]; and National Institutes of Health National Center for Research Resources [Grant RR-021940].

Person to receive reprint requests: Dr. Hong Lu, Department of Pharmacology, SUNY Upstate Medical University, 750 E Adams ST, Syracuse, NY 13210. Email: luh@upstate.edu.

Downloaded from dmd.aspetjournals.org at ASPET Journals on April 18, 2024

DMD Fast Forward. Published on February 4, 2013 as DOI: 10.1124/dmd.112.050211
This article has not been copyedited and formatted. The final version may differ from this version.

Figure Legends:

FIG. 1. Hepatic ontogeny of total transcripts of Phase-II enzymes in male C57BL/6J mice. Livers from C57BL/6J mice of ages from Day-2 to Day60 were used for RNA-seq quantification of (A) Uridine diphosphate-glucuronosyltransferases (Ugts), (B) Sulfotransferases (Sults), (C) Glutathione *S*-transferases (Gsts), (D) N-acetyltransferases (Nats), (E) Methyltransferases, and (F) enzymes for amino acid (AA) conjugation. Y-axis represents mRNAs expressed as fragments per kilobase of exon per million reads mapped (FPKM). N=3, mean ± SE. * $p < 0.05$ versus Day -2.

FIG. 2. Hierarchical clustering of hepatic ontogeny of Phase-II conjugating enzymes in male C57BL/6J mice. Livers from C57BL/6J mice of ages from Day-2 to Day60 were used for RNA-seq quantification. The two trees describe the relationship between different gene expression profiles (right tree) and various ages (bottom tree). The dendrogram scale represents the correlation distances. Average FPKM values of three replicates per age are given by colored squares: red, relatively high expression; blue, relatively low expression. The solid lines separate the expression profiles into three groups of perinatal-, adolescent-, and adult-predominant expression.

FIG. 3. Hepatic ontogeny of Ugt mRNAs in male C57BL/6J mice. Livers from C57BL/6J mice of ages from Day-2 to Day60 were used for RNA-seq quantification. (A) Y-axis represents mRNAs expressed as fragments per kilobase of exon per million reads mapped (FPKM). N=3, mean ± SE. (B) Pie chart represents relative mRNA expression of each Ugt isoform as the percentage of total Ugt transcripts.

Downloaded from dmd.aspetjournals.org at ASPET Journals on April 18, 2024

DMD Fast Forward. Published on February 4, 2013 as DOI: 10.1124/dmd.112.050211
This article has not been copyedited and formatted. The final version may differ from this version.

FIG. 4. Hepatic ontogeny of Sult mRNAs in male C57BL/6J mice. Livers from C57BL/6J mice of ages from Day-2 to Day60 were used for RNA-seq quantification. (A) Y-axis represents mRNAs expressed as fragments per kilobase of exon per million reads mapped (FPKM). N=3, mean ± SE. (B) Pie chart represents relative mRNA expression of each Sult isoform as the percentage of total Sult transcripts.

FIG. 5. Hepatic ontogeny of Gst mRNAs in male C57BL/6J mice. Livers from C57BL/6J mice of ages from Day-2 to Day60 were used for RNA-seq quantification. (A) Y-axis represents mRNAs expressed as fragments per kilobase of exon per million reads mapped (FPKM). N=3, mean ± SE. (B) Pie chart represents relative mRNA expression of each Gst isoform as the percentage of total Gst transcripts.

FIG. 6. Hepatic ontogeny of transcripts of Nats, methyltransferases, and AA conjugating enzymes in male C57BL/6J mice. Livers from C57BL/6J mice of ages from Day-2 to Day60 were used for RNA-seq quantification. Y-axis represents mRNAs expressed as fragments per kilobase of exon per million reads mapped (FPKM). N=3, mean ± SE.

FIG. 7. Hepatic ontogeny of mRNAs of genes encoding enzymes for the synthesis of co-substrates for Phase-II conjugation in male C57BL/6J mice. Livers from C57BL/6J mice of ages from Day-2 to Day60 were used for RNA-seq quantification. Y-axis represents mRNAs expressed as fragments per kilobase of exon per million reads mapped (FPKM). N=3, mean ± SE.

FIG. 8. Tissue distribution of mRNAs of genes encoding Ugts and Sults in adult male C57BL/6J mice. (A) Pie chart represents relative mRNA expression of each Ugt isoform as the percentage of total Ugt transcripts in liver, kidney, and small

Downloaded from dmd.aspetjournals.org at ASPET Journals on April 18, 2024

DMD Fast Forward. Published on February 4, 2013 as DOI: 10.1124/dmd.112.050211
This article has not been copyedited and formatted. The final version may differ from this version.

intestine, respectively, from C57BL/6J mice of 60 days old. N=2, mean. (B) Pie chart represents relative mRNA expression of each Sult isoform as the percentage of total Sult transcripts in liver, kidney, and small intestine, respectively, from C57BL/6J mice of 60 days old. N=2, mean.

FIG. 9. Tissue distribution of mRNAs of genes encoding Gsts in adult male C57BL/6J mice. Pie chart represents relative mRNA expression of each Gst isoform as the percentage of total Gst transcripts in liver, kidney, and small intestine, respectively, from C57BL/6J mice of 60 days old. N=2, mean.

FIG. 10. Tissue distribution of mRNAs of genes encoding other Phase-II enzymes and enzymes responsible for the synthesis of co-substrates for Phase-II conjugation reaction in adult male C57BL/6J mice. (A) and (B) Stacked column chart represents relative mRNA expression of each Phase-II enzyme as the percentage of total transcripts of this enzyme in liver, kidney, and small intestine from C57BL/6J mice of 60 days old. N=2, mean. (C) Stacked column chart represents relative mRNA expression of each co-substrate-synthesizing enzyme as the percentage of total transcripts of this enzyme in liver, kidney, and small intestine from C57BL/6J mice of 60 days old. N=2, mean.

FIG. 11. Real-Time PCR validation of RNA-seq data of ontogenic mRNA expression of mGst3 and Nat8 in livers of male C57BL/6J mice. Total RNAs from livers of male C57BL/6J mice of ages of Day -2, 1, 5, 10, 20, 25, 45, and 60 were used for Real-time PCR validation. N=3, mean ± SE. Y-axis represents mRNAs calculated by the comparative CT method, which determines the amount of target

Downloaded from dmd.aspetjournals.org at ASPET Journals on April 18, 2024

DMD Fast Forward. Published on February 4, 2013 as DOI: 10.1124/dmd.112.050211
This article has not been copyedited and formatted. The final version may differ from this version.

normalized to the geometric mean of Gapdh and Ncu-g1. * $p < 0.05$ versus Day -2.

Downloaded from dmd.aspetjournals.org at ASPET Journals on April 18, 2024

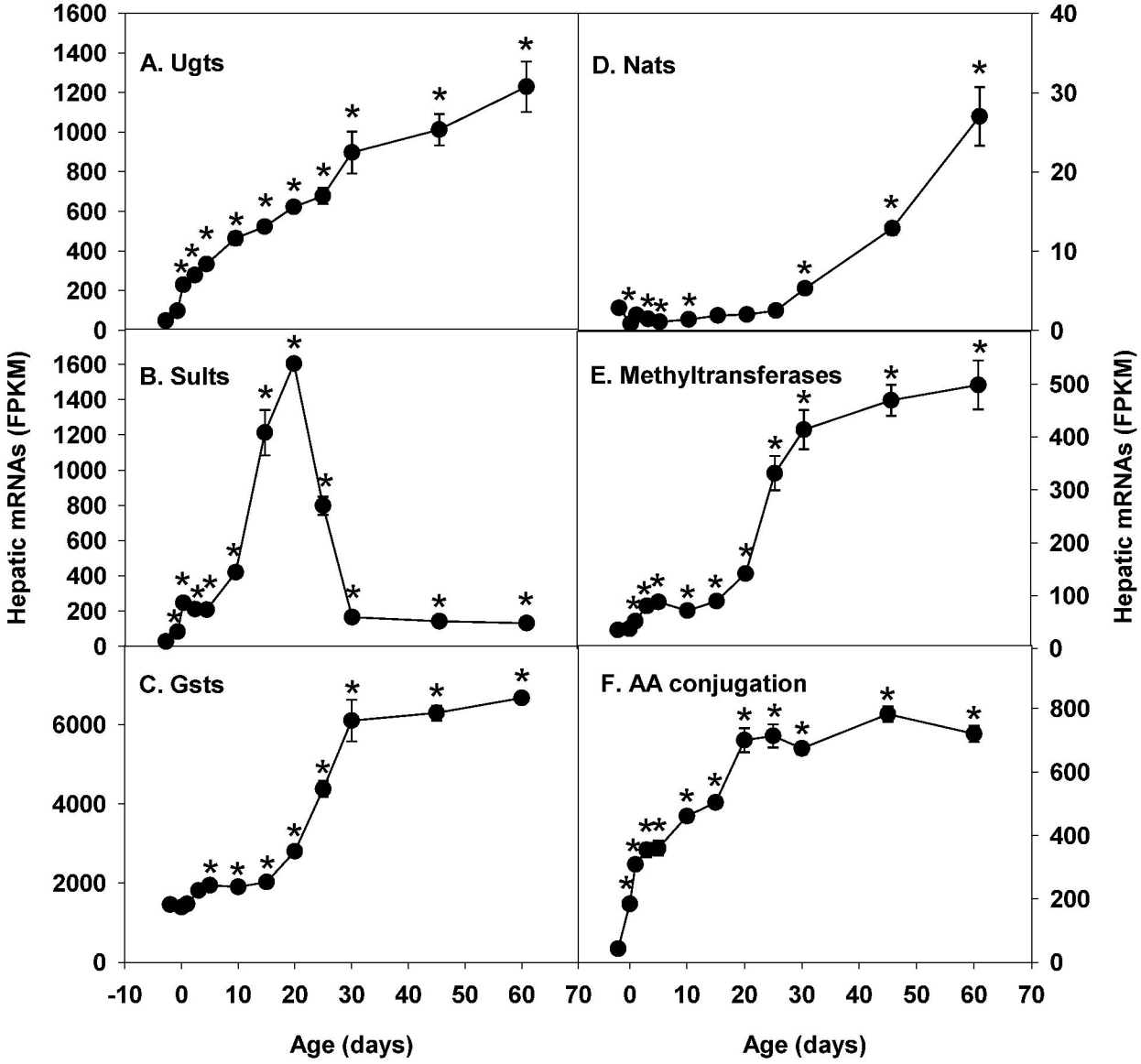
A. Ugts
B. Sults
C. Gsts
D. Nats
E. Methyltransferases
F. AA conjugation
Hepatic mRNAs (FPKM)
Hepatic mRNAs (FPKM)
Age (days)
Age (days)

Fig. 1

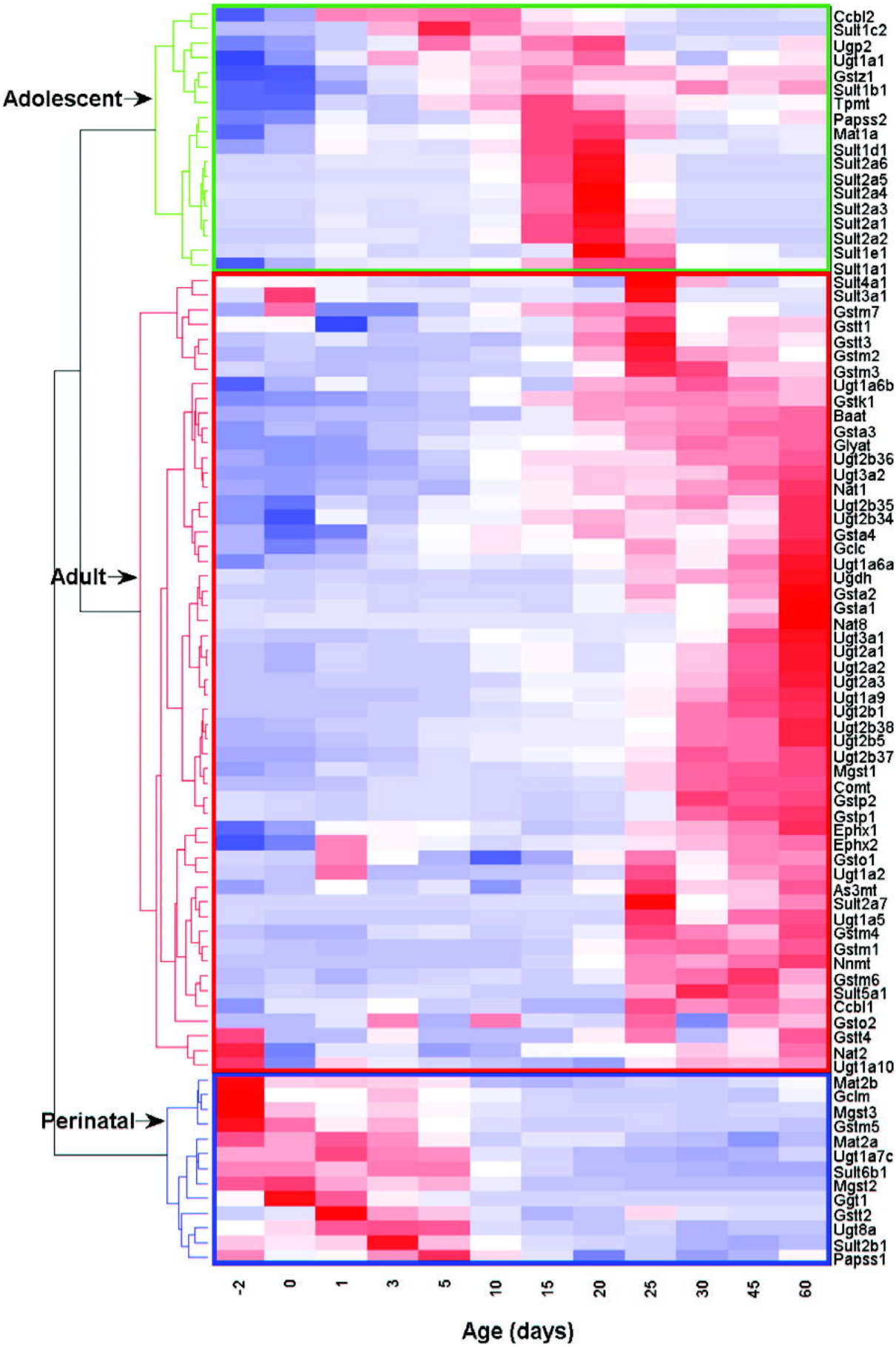
Adolescent
Adult
Perinatal
Ccbl2
Sult1c2
Ugp2
Ugt1a1
Gstz1
Sult1b1
Tpmt
Papss2
Mat1a
Sult1d1
Sult2a6
Sult2a5
Sult2a4
Sult2a3
Sult2a1
Sult2a2
Sult1e1
Sult1a1
Sult4a1
Sult3a1
Gstm7
Gstt1
Gstt3
Gstm2
Gstm3
Ugt1a6b
Gstk1
Baat
Gsta3
Glyat
Ugt2b36
Ugt3a2
Nat1
Ugt2b35
Ugt2b34
Gsta4
Gclc
Ugt1a6a
Ugdh
Gsta2
Gsta1
Nat8
Ugt3a1
Ugt2a1
Ugt2a2
Ugt2a3
Ugt1a9
Ugt2b1
Ugt2b38
Ugt2b5
Ugt2b37
Mgst1
Comt
Gstp2
Gstp1
Ephx1
Ephx2
Gsto1
Ugt1a2
As3mt
Sult2a7
Ugt1a5
Gstm4
Gstm1
Nnmt
Gstm6
Sult5a1
Ccbl1
Gsto2
Gstt4
Nat2
Ugt1a10
Mat2b
Gclm
Mgst3
Gstm5
Mat2a
Ugt1a7c
Sult6b1
Mgst2
Ggt1
Gstt2
Ugt8a
Sult2b1
Papss1
-2
0
1
3
5
10
15
20
25
30
45
60
Age (days)

Fig. 2

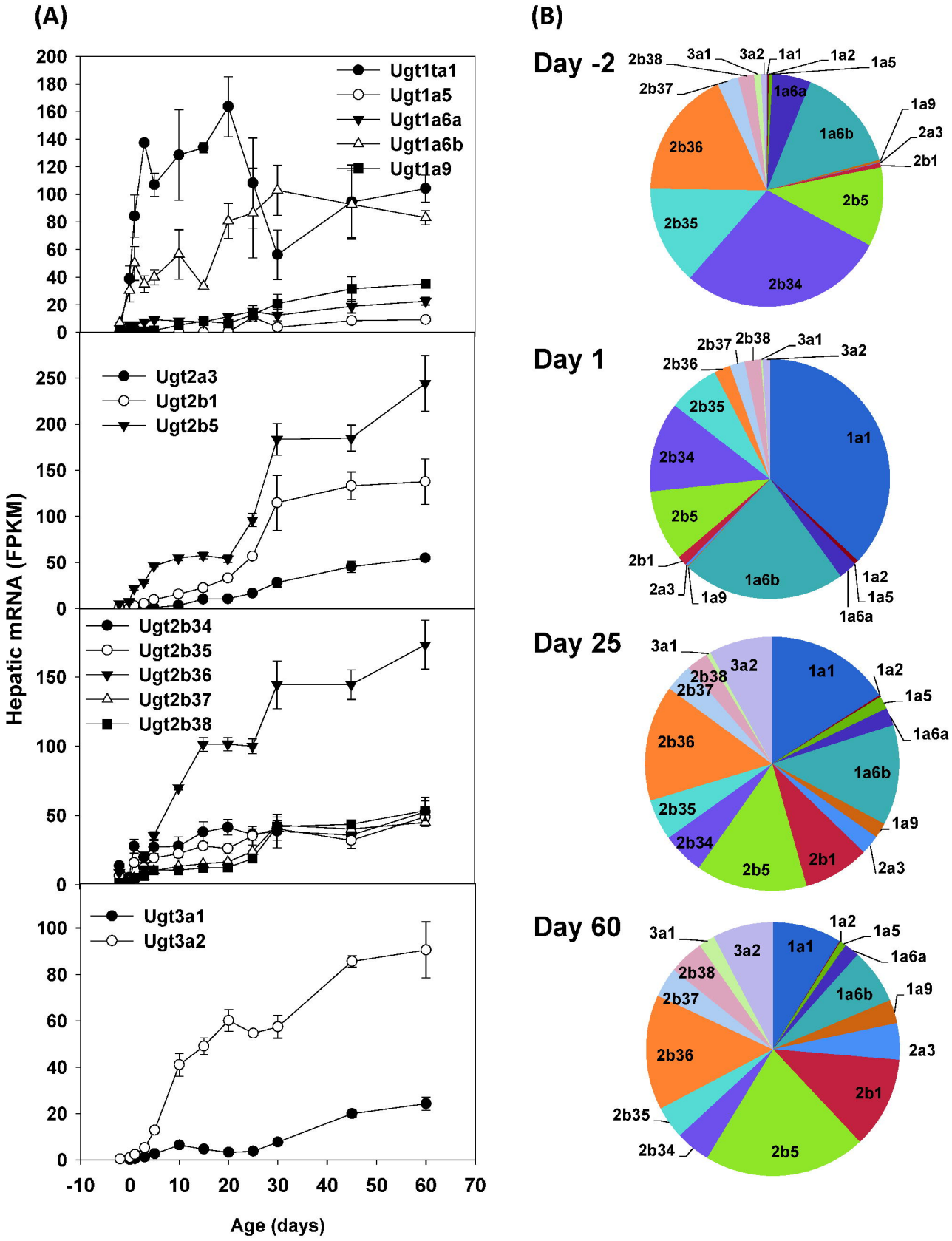
(A)
(B)
Hepatic mRNA (FPKM)
Age (days)
Ugt1ta1
Ugt1a5
Ugt1a6a
Ugt1a6b
Ugt1a9
Ugt2a3
Ugt2b1
Ugt2b5
Ugt2b34
Ugt2b35
Ugt2b36
Ugt2b37
Ugt2b38
Ugt3a1
Ugt3a2
Day -2
Day 1
Day 25
Day 60

Fig. 3

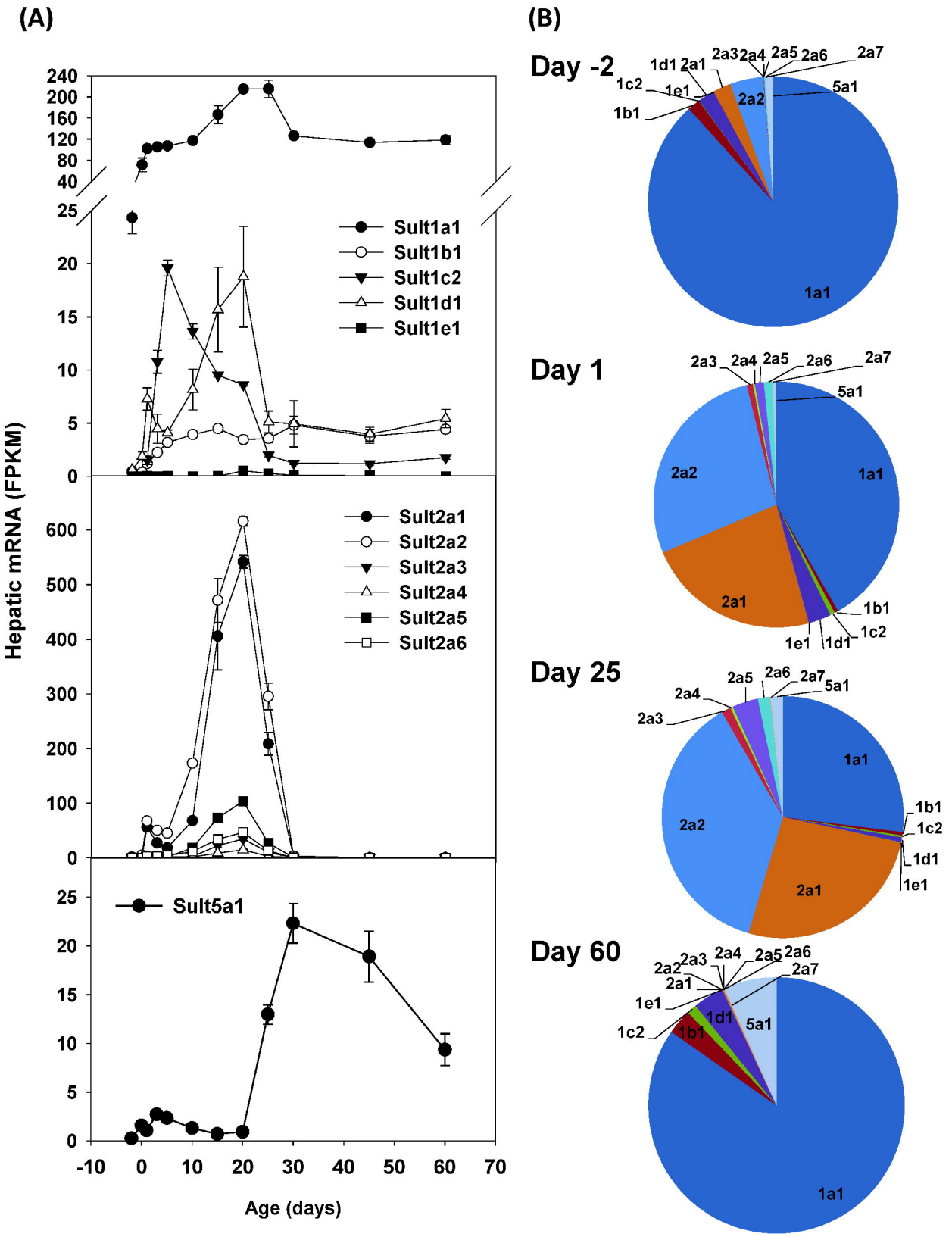
(A)
(B)
Hepatic mRNA (FPKM)
Age (days)
Sult1a1
Sult1b1
Sult1c2
Sult1d1
Sult1e1
Sult2a1
Sult2a2
Sult2a3
Sult2a4
Sult2a5
Sult2a6
Sult5a1
Day -2
Day 1
Day 25
Day 60
1a1
2a1
2a2
2a3
2a4
2a5
2a6
2a7
5a1
1b1
1c2
1d1
1e1

Fig. 4

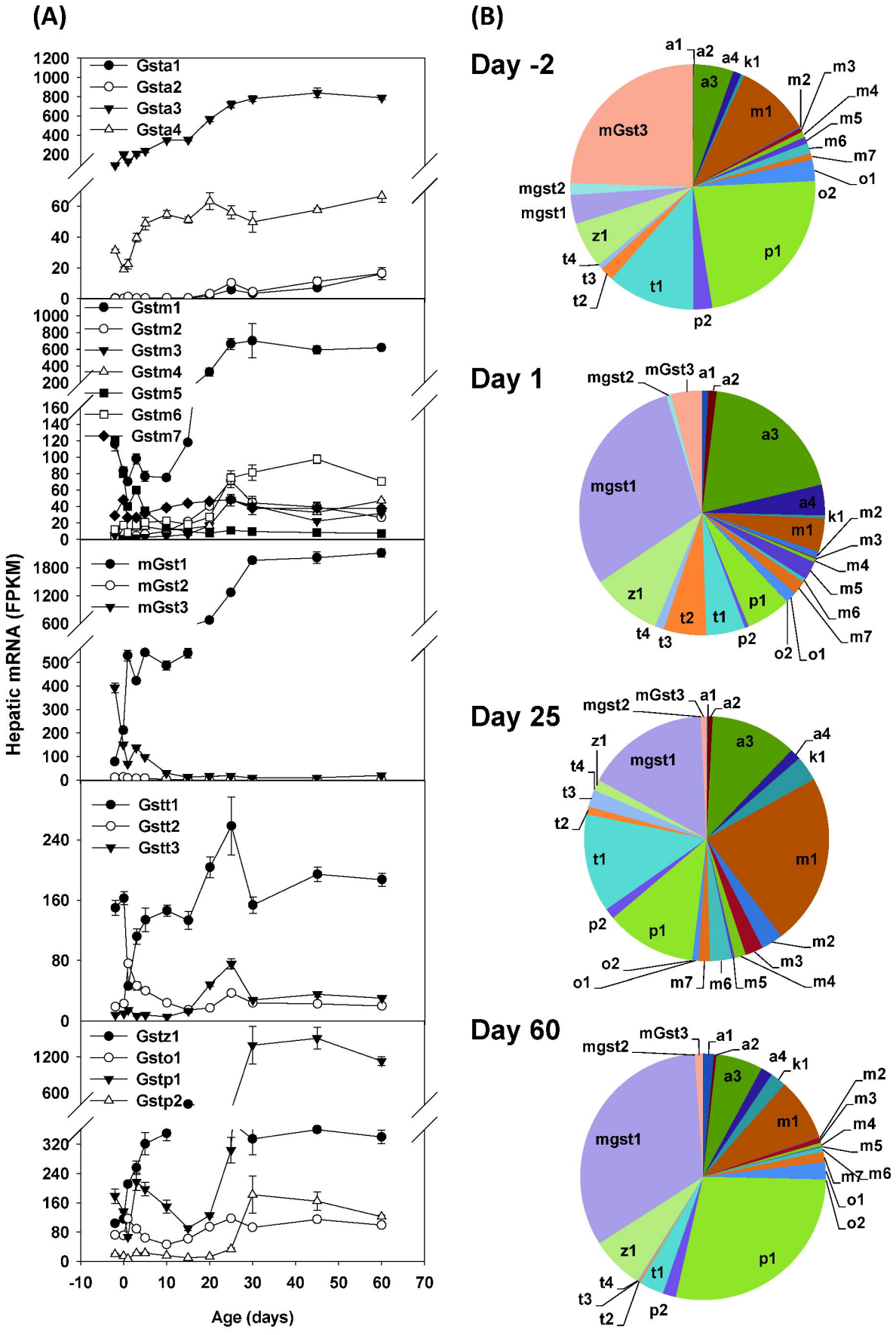
(A)
(B)
Hepatic mRNA (FPKM)
Gsta1
Gsta2
Gsta3
Gsta4
Gstm1
Gstm2
Gstm3
Gstm4
Gstm5
Gstm6
Gstm7
mGst1
mGst2
mGst3
Gstt1
Gstt2
Gstt3
Gstz1
Gsto1
Gstp1
Gstp2
Age (days)
Day -2
Day 1
Day 25
Day 60
a1
a2
a3
a4
k1
m1
m2
m3
m4
m5
m6
m7
mGst3
mgst2
mgst1
o1
o2
p1
p2
t1
t2
t3
t4
z1

Fig. 5

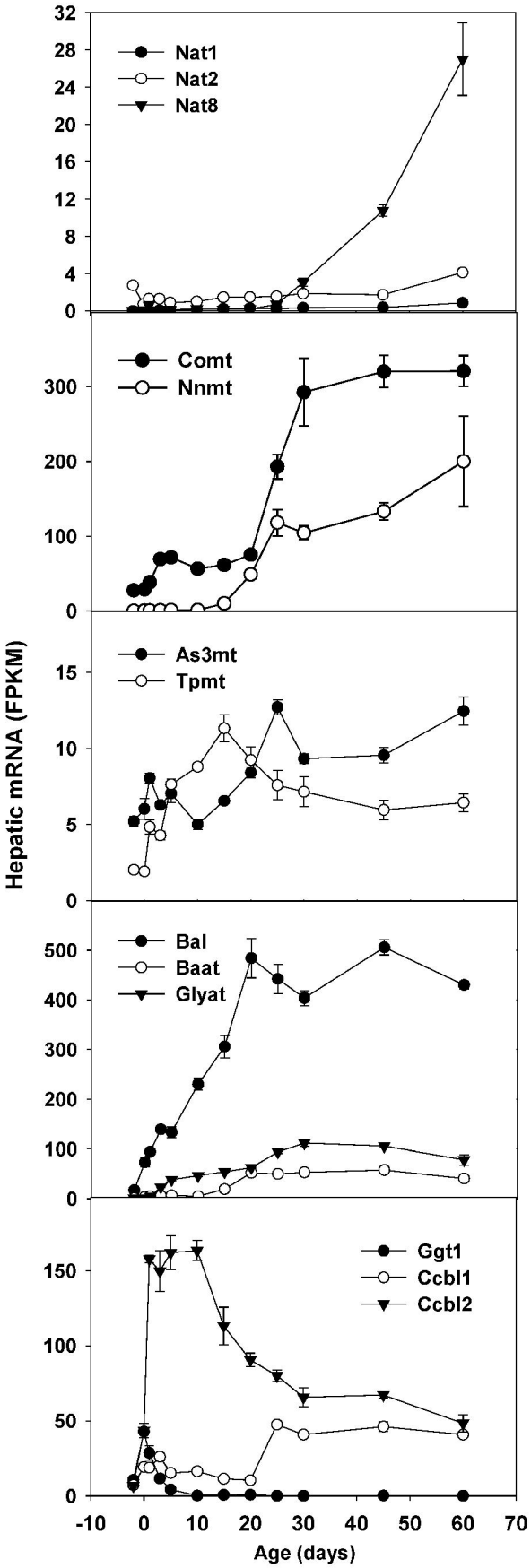
Hepatic mRNA (FPKM)
Nat1
Nat2
Nat8
Comt
Nnmt
As3mt
Tpmt
Bal
Baat
Glyat
Ggt1
Ccbl1
Ccbl2
Age (days)

Fig. 6

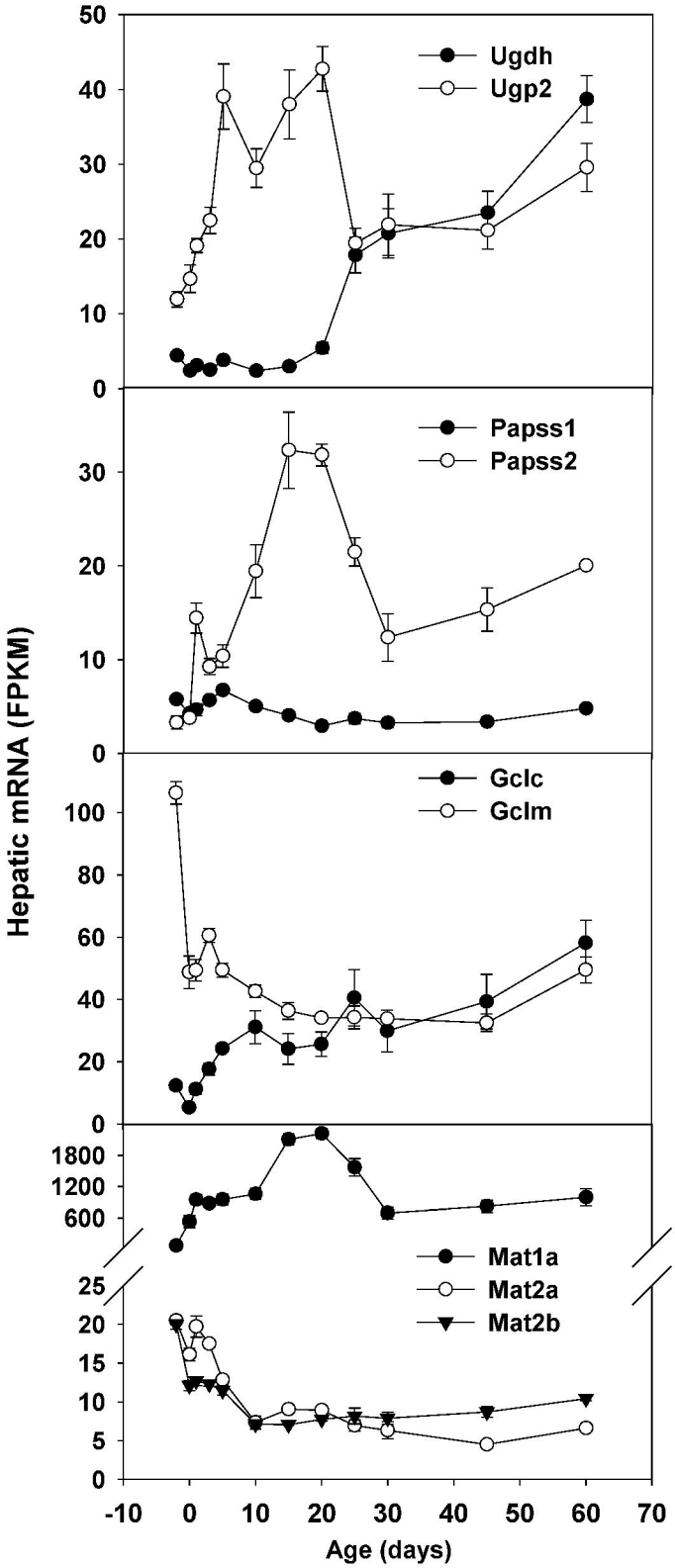
Hepatic mRNA (FPKM)
Ugdh
Ugp2
Papss1
Papss2
Gclc
Gclm
Mat1a
Mat2a
Mat2b
Age (days)

Fig. 7

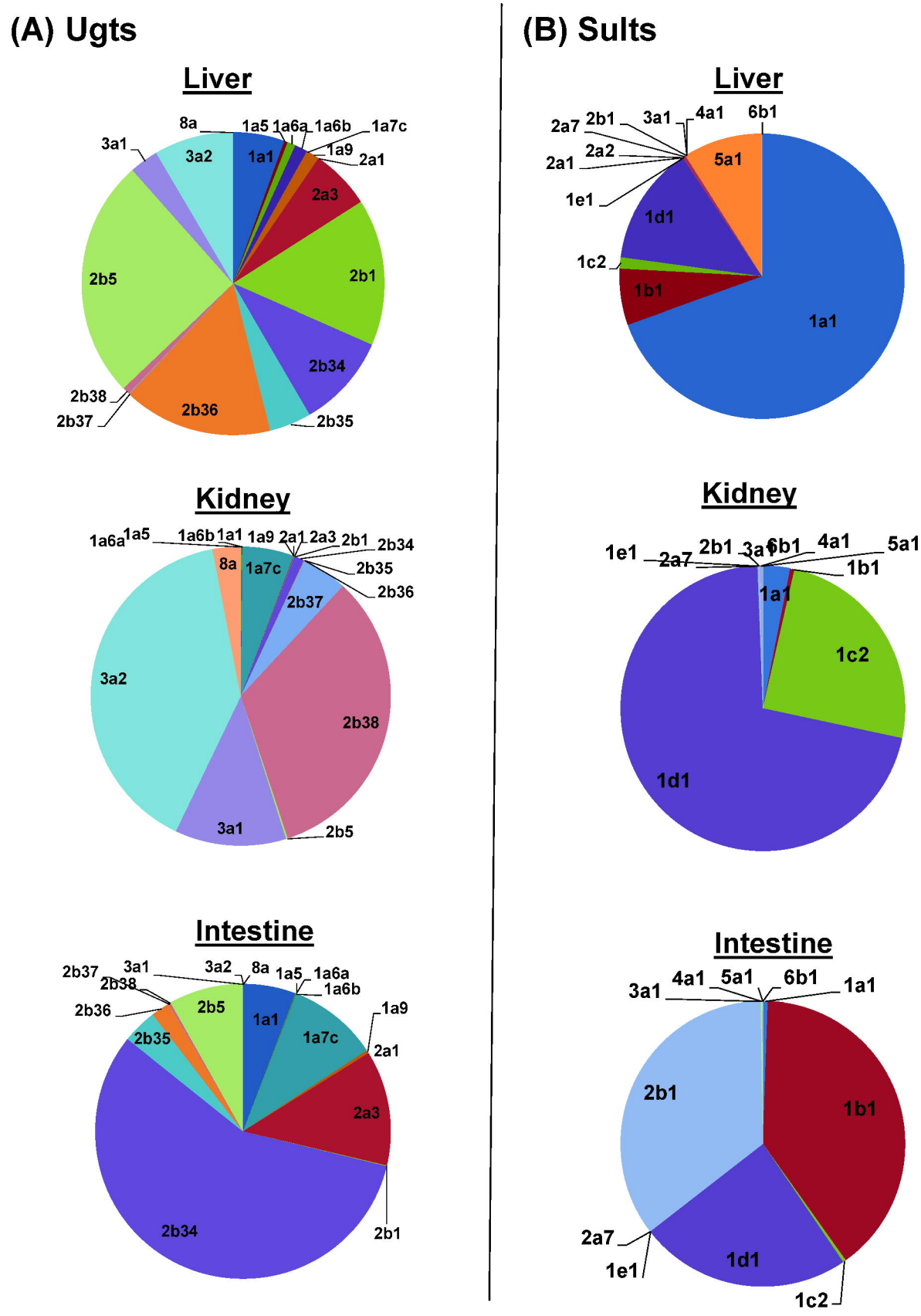
(A) Ugts
Liver
8a
1a5
1a6a
1a6b
1a7c
3a1
3a2
1a1
1a9
2a1
2a3
2b5
2b1
2b34
2b38
2b36
2b37
2b35
Kidney
1a6a
1a5
1a6b
1a1
1a9
2a1
2a3
2b1
2b34
8a
1a7c
2b35
2b36
2b37
3a2
2b38
3a1
2b5
Intestine
2b37
3a1
3a2
8a
1a5
1a6a
1a6b
2b38
2b36
2b5
1a1
1a9
2b35
1a7c
2a1
2a3
2b34
2b1
(B) Sults
Liver
2a7
2b1
3a1
4a1
6b1
2a1
2a2
5a1
1e1
1d1
1c2
1b1
1a1
Kidney
1e1
2a7
2b1
3a1
6b1
4a1
5a1
1b1
1a1
1c2
1d1
Intestine
3a1
4a1
5a1
6b1
1a1
2b1
1b1
2a7
1d1
1e1
1c2

Fig. 8

Liver

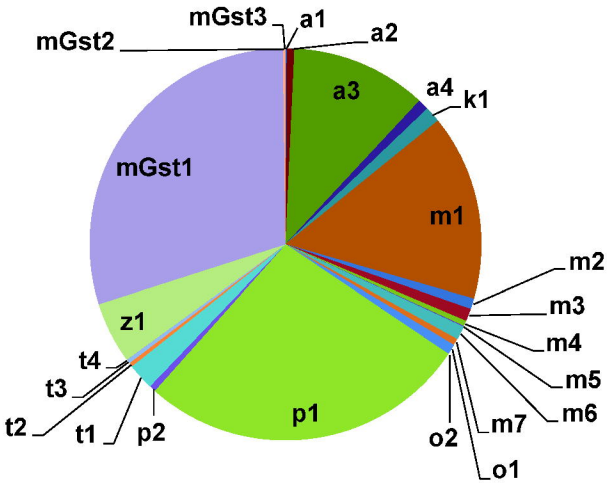

Kidney

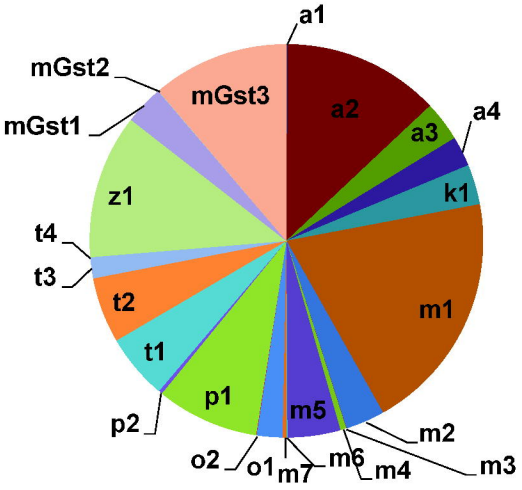

Intestine

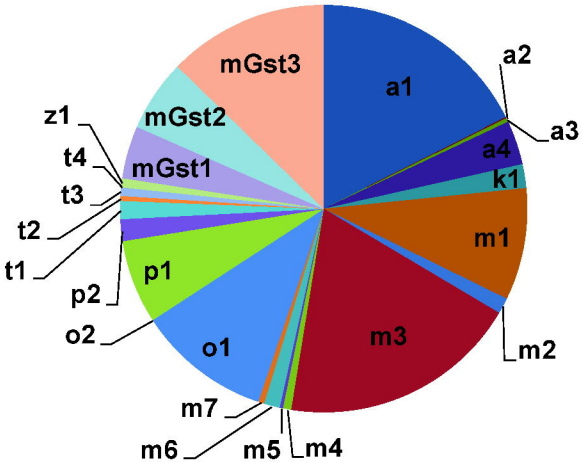

Fig. 9

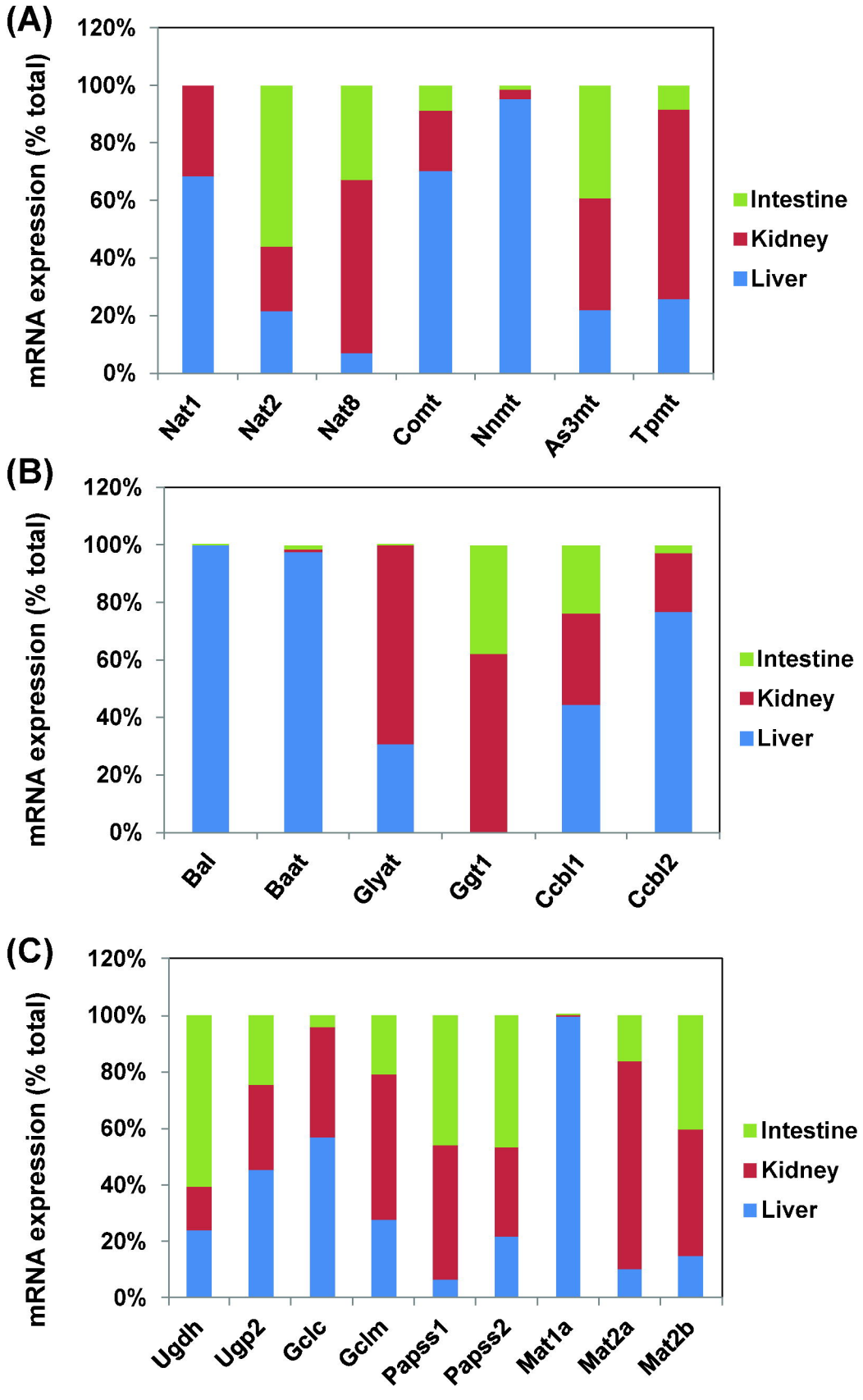
(A)
mRNA expression (% total)
120%
100%
80%
60%
40%
20%
0%
Nat1
Nat2
Nat8
Comt
Nnmt
As3mt
Tpmt
Intestine
Kidney
Liver
(B)
mRNA expression (% total)
120%
100%
80%
60%
40%
20%
0%
Bal
Baat
Glyat
Ggt1
Ccbl1
Ccbl2
Intestine
Kidney
Liver
(C)
mRNA expression (% total)
120%
100%
80%
60%
40%
20%
0%
Ugdh
Ugp2
Gclc
Gclm
Papss1
Papss2
Mat1a
Mat2a
Mat2b
Intestine
Kidney
Liver

Fig. 10

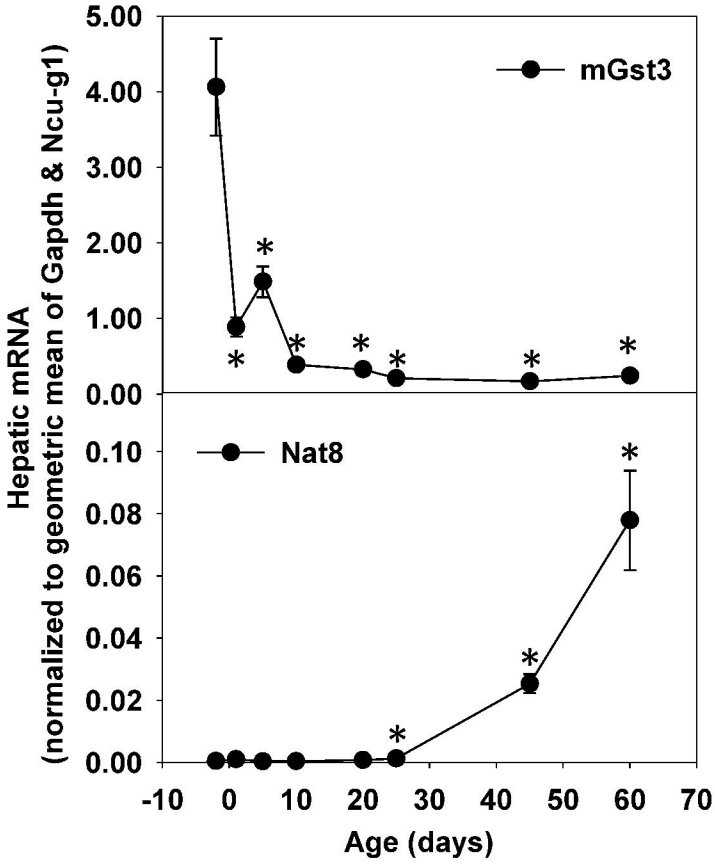
Hepatic mRNA
(normalized to geometric mean of Gapdh & Ncu-g1)
mGst3
Nat8
5.00
4.00
3.00
2.00
1.00
0.00
0.10
0.08
0.06
0.04
0.02
0.00
-10
0
10
20
30
40
50
60
70
Age (days)

Fig. 11